

# FINITE ELEMENT CONVERGENCE FOR STATE-BASED PERIDYNAMIC FRACTURE MODELS\*

PRASHANT K. JHA <sup>†</sup> AND ROBERT LIPTON <sup>‡</sup>

**Abstract.** We establish the a-priori convergence rate for finite element approximations of a class of nonlocal nonlinear fracture models. We consider state based peridynamic models where the force at a material point is due to both the strain between two points and the change in volume inside the domain of nonlocal interaction. The pairwise interactions between points are mediated by a bond potential of multi-well type while multi point interactions are associated with volume change mediated by a hydrostatic strain potential. The hydrostatic potential can either be a quadratic function, delivering a linear force-strain relation, or a multi-well type that can be associated with material degradation and cavitation. We first show the well-posedness of the peridynamic formulation and that peridynamic evolutions exist in the Sobolev space  $H^2$ . We show that the finite element approximations converge to the  $H^2$  solutions uniformly as measured in the mean square norm. For linear continuous finite elements the convergence rate is shown to be  $C_t \Delta t + C_s h^2 / \epsilon^2$ , where  $\epsilon$  is the size of horizon,  $h$  is the mesh size, and  $\Delta t$  is the size of time step. The constants  $C_t$  and  $C_s$  are independent of  $\Delta t$  and  $h$  and may depend on  $\epsilon$  through the norm of the exact solution. We demonstrate the stability of the semi-discrete approximation. The stability of the fully discrete approximation is shown for the linearized peridynamic force. We present numerical simulations with dynamic crack propagation that support the theoretical convergence rate.

**Key words.** Nonlocal fracture models, peridynamic, state based peridynamic, numerical analysis, finite element approximation

**AMS subject classifications.** 34A34, 34B10, 74H55, 74S05

**1. Introduction.** In this work, we study the state-based peridynamic theory and obtain an a-priori error bound for the finite element approximation. The peridynamic theory is a reformulation of classical continuum mechanics carried out in the work of Silling in [Silling, 2000, Silling et al., 2007]. The strain inside the medium is expressed in terms of displacement differences as opposed to the displacement gradients. Acceleration of a point is now due to the sum of the forces acting on the point from near by points. The new kinematics bypasses the difficulty incurred by juxtaposing displacement gradients and discontinuities as in the case of classical fracture theories. The nonlocal fracture theory has been applied numerically to model the complex fracture phenomenon in materials, see [Weckner and Abeyaratne, 2005], [Silling and Bobaru, 2005], [Silling and Lehoucq, 2008], [Silling et al., 2010], [Foster et al., 2011], [Ha and Bobaru, 2010], [Agwai et al., 2011], [Bobaru and Hu, 2012], [Ghajari et al., 2014], [Du et al., 2013a], [Lipton et al., 2016]. Every point interacts with its neighbors inside a ball of fixed radius called the horizon. The size of horizon sets the length scale of nonlocal interaction. When the forces between points are linear and nonlocal length scale tends to zero, it is seen that peridynamic models converge to the classic model of linear elasticity, [Emmrich et al., 2013, Silling and Lehoucq, 2008, Aksoylu and Unlu, 2014, Mengesha and Du, 2015]. The work of [Tian and Du, 2014] provides an analytic framework for analyzing FEM for linear bond and state-based peridynamics. For nonlinear forces associated with double well potentials the peridynamic evolution converges in the small horizon limit to an evolution with a sharp evolving fracture set and the evolution is governed by the classic linear elastic wave equation away from the fracture

---

\***Funding:** This material is based upon work supported by the U. S. Army Research Laboratory and the U. S. Army Research Office under contract/grant number W911NF1610456.

<sup>†</sup>Department of Mathematics, Louisiana State University, Baton Rouge, LA ([prashant.j16o@gmail.com](mailto:prashant.j16o@gmail.com)).  
Orcid: <https://orcid.org/0000-0003-2158-364X>

<sup>‡</sup>Department of Mathematics, Louisiana State University, Baton Rouge, LA ([lipton@math.lsu.edu](mailto:lipton@math.lsu.edu)).  
Orcid: <https://orcid.org/0000-0002-1382-3204>

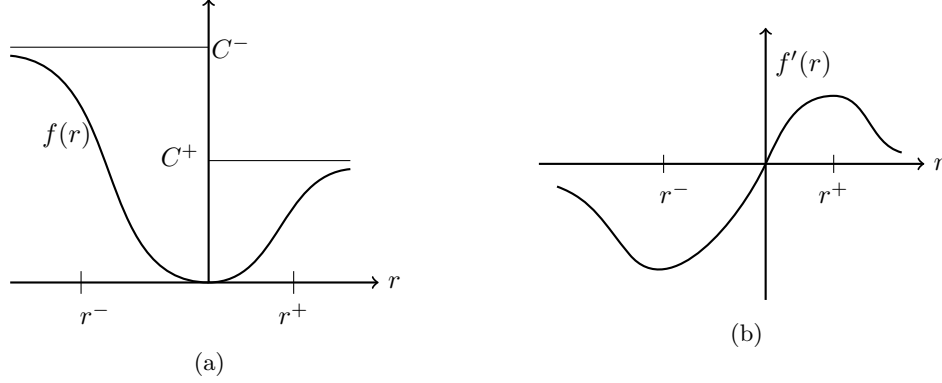


Fig. 1: (a) Potential function  $f(r)$  for tensile force.  $C^+$  and  $C^-$  are two extreme values of  $f$ . (b) Cohesive tensile force.

set, see [Lipton, 2016, Lipton, 2014, Jha and Lipton, 2018a]. A recent review of the state of the art can be found in [Bobaru et al., 2016] and [Du, 2018a].

In this work we assume small deformation and work with linearized bond-strain. Let  $D \subset \mathbb{R}^d$ , for  $d = 2, 3$ , be the material domain. For a displacement field  $\mathbf{u} : D \times [0, T] \rightarrow \mathbb{R}^d$ , the bond-strain between two material points  $\mathbf{x}, \mathbf{y} \in D$  is given by

$$(1) \quad S(\mathbf{y}, \mathbf{x}, t; \mathbf{u}) = \frac{\mathbf{u}(\mathbf{y}, t) - \mathbf{u}(\mathbf{x}, t)}{|\mathbf{y} - \mathbf{x}|} \cdot \frac{\mathbf{y} - \mathbf{x}}{|\mathbf{y} - \mathbf{x}|}.$$

Let  $\epsilon > 0$  be the size of horizon and  $H_\epsilon(\mathbf{x}) = \{\mathbf{y} \in \mathbb{R}^d : |\mathbf{y} - \mathbf{x}| < \epsilon\}$  be the neighborhood of a material point  $\mathbf{x}$ . For pairwise interaction, we assume the following form of pairwise interaction potential

$$(2) \quad \mathcal{W}^\epsilon(S(\mathbf{y}, \mathbf{x}, t; \mathbf{u})) = \frac{J^\epsilon(|\mathbf{y} - \mathbf{x}|)}{\epsilon|\mathbf{y} - \mathbf{x}|} f(\sqrt{|\mathbf{y} - \mathbf{x}|} S(\mathbf{y}, \mathbf{x}, t; \mathbf{u})),$$

where  $J^\epsilon(|\mathbf{y} - \mathbf{x}|)$  is the influence function. We assume  $J^\epsilon(|\mathbf{y} - \mathbf{x}|) = J(|\mathbf{y} - \mathbf{x}|/\epsilon)$  where  $0 \leq J(r) \leq M$  for  $r < 1$  and  $J(r) = 0$  for  $r \geq 1$ . The potential  $f$ , see Figure 1a, is assumed to be convex for small strains and becomes concave for larger strains. In the widely used prototypical micro-elastic brittle (PMB) peridynamic material, the strain vs force profile is linear up to some critical strain  $S_c$  and is zero for any strain above  $S_c$ . In contrast, the peridynamic force given by  $\partial_S \mathcal{W}^\epsilon$ , is linear near zero strain and as the strain gets larger and reaches the critical strain,  $S_c^+$  ( $S_c^-$ ) for positive (negative) strain, the bond starts to soften, see Figure 1b. For a given potential function  $f$ , the critical strain is given by  $S_c^+ = \frac{r^+}{\sqrt{|\mathbf{y} - \mathbf{x}|}}$  and  $S_c^- = \frac{r^-}{\sqrt{|\mathbf{y} - \mathbf{x}|}}$  where  $r^+ > 0, r^- < 0$  are the inflection points of the potential function  $f$  as shown in Figure 1a.

The spherical or hydrostatic strain  $\theta(\mathbf{x}, t; \mathbf{u})$  at material point is given by

$$(3) \quad \theta(\mathbf{x}, t; \mathbf{u}) = \frac{1}{\epsilon^d \omega_d} \int_{H_\epsilon(\mathbf{x})} J^\epsilon(|\mathbf{y} - \mathbf{x}|) S(\mathbf{y}, \mathbf{x}, t; \mathbf{u}) |\mathbf{y} - \mathbf{x}| d\mathbf{y},$$

where  $\omega_d$  is the volume of unit ball in dimension  $d = 2, 3$ . The potential for hydrostatic

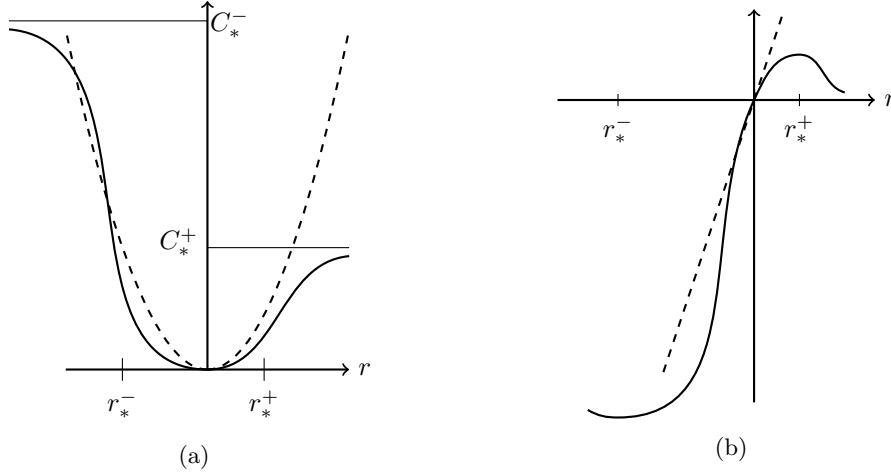


Fig. 2: (a) Two types of potential function  $g(r)$  for hydrostatic force. Dashed line corresponds to the quadratic potential  $g(r) = \beta r^2/2$ . Solid line corresponds to the convex-concave type potential  $g(r)$ . For the convex-concave type potential, there are two special points  $r_*^-$  and  $r_*^+$  at which material points start to soften.  $C_*^+$  and  $C_*^-$  are two extreme values. (b) Hydrostatic forces.

interaction is of the form

$$(4) \quad \mathcal{V}^\epsilon(\theta(\mathbf{x}, t; \mathbf{u})) = \frac{g(\theta(\mathbf{x}, t; \mathbf{u}))}{\epsilon^2},$$

where  $g$  is the potential function associated to hydrostatic strain. Here  $g$  can be of two types: 1) a quadratic function with only one well at zero strain, and 2) a convex-concave function with a wells at the origin and at  $\pm\infty$ , see Figure 2a. If  $g$  is assumed to be quadratic then the force due to spherical strain is linear. If  $g$  is a multi-well potential, the material softens as the hydrostatic strains exceeds critical value. For the convex-concave type  $g$ , the critical values are  $0 < \theta_c^+$  and  $\theta_c^- < 0$  beyond which the force begins to soften is related to the inflection point  $r_*^+$  and  $r_*^-$  of  $g$  as follows

$$(5) \quad \theta_c^+ = r_*^+, \quad \theta_c^- = r_*^-.$$

The critical compressive hydrostatic strain where the force begins to soften for negative hydrostatic strain is chosen much larger in magnitude than  $\theta_c^+$ , i.e.  $\theta_c^+ \ll |\theta_c^-|$ .

The finite element approximation has been applied to peridynamic fracture, however there remains a paucity of literature addressing the rigorous a-priori convergence rate of the finite element approximation to peridynamic problems in the presence of material failure. This aspect provides the motivation for the present work. In this paper we first prove existence of peridynamic evolutions taking values in  $H^2(D; \mathbb{R}^d) \cap H_0^1(D; \mathbb{R}^d)$  that are twice differentiable in time, see Theorem 2. We note that as these evolutions will become more fracture like as the region of nonlocal interaction decreases. These evolutions can be thought of as inner approximations to fracture evolutions. On passing to subsequences it is possible to show that the  $H^2(D; \mathbb{R}^d) \cap H_0^1(D; \mathbb{R}^d)$  evolutions converge in the limit of vanishing non-locality to a limit solution taking values in the space of special functions of bounded deformation SBD. Here the limit evolution has a well defined Griffith fracture energy bounded

by the initial data, see [Lipton, 2016] and [Jha and Lipton, 2019]. We show here that higher temporal regularity can be established if the body force changes smoothly in time. Motivated by these considerations we develop finite element error estimates for solutions that take values in  $H^2(D; \mathbb{R}^d) \cap H_0^1(D; \mathbb{R}^d)$  and for a bounded time interval.

In this paper we obtain an a-priori  $L^2$  error bound for the finite element approximation of the displacement and velocity using a central in time discretization. Due to the nonlinear nature of the problem we get a convergence rate by using Lax Richtmyer stability together with consistency. Both stability and consistency are shown to follow from the Lipschitz continuity of the peridynamic force in  $L^2(D; \mathbb{R}^d)$ , see section 4.2.1 and section 4.2.2. The bound on the  $L^2$  error is uniform in time and is given by  $C_t \Delta t + C_s h^2 / \epsilon^2$ , where the constants  $C_t$  and  $C_s$  are independent of  $\Delta t$  and mesh size  $h$ , see Theorem 6. A more elaborate discussion of the a-priori bound is presented in section subsection 4.2. For the linearized model we obtain a stability condition on  $\Delta t$ , Theorem 9, that is of the same form as those given for linear local and nonlocal wave equations [Karaa, 2012, Guan and Gunzburger, 2015]. We demonstrate stability for the linearized model noting that for small strains the material behaves like a linear elastic material and that the stability of the linearized model is necessary for the stability of nonlinear model. We believe a more constructive CFL stability condition is possible for the linear case and will pursue this in future work.

Previous work [Jha and Lipton, 2018a] treated spatially Lipschitz continuous solutions and addressed the finite difference approximation and obtained bounds on the  $L^2$  error for the displacement and velocity that are uniform in time and of the form  $C_t \Delta t + C_s h / \epsilon^2$ , where constants the  $C_t$  and  $C_s$  are as before. For finite elements the convergence rate is seen to be slower than for the FEM model introduced here and is of order  $h / \epsilon^2$  as opposed to  $h^2 / \epsilon^2$ . On the other hand the FEM method increases the computational work due to the inversion of the mass matrix.

We carry out numerical experiments for dynamic crack propagation and obtain convergence rates for Plexiglass that are in line with the theory, see section 5. We also compare the Griffith’s fracture energy with the peridynamic energy of the material softening zone we show good agreement between the two energies, see subsection 5.2. Finite difference methods are less expensive than finite element approximations for nonlocal problems, however the latter offers more control on the accuracy of solution see, [Macek and Silling, 2007, Littlewood, 2010, Du et al., 2013c, Gerstle et al., 2007, Du, 2018b].

Here the a-priori  $L^2$  convergence rates for the FEM given by Theorem 6 include the effects of material degradation through the softening of material properties. The FEM simulations presented in this paper show that the material develops localized softening zones (region where bonds exceed critical tensile strain) as it deforms. This is in contrast to linear peridynamic models which are incapable of developing softening zones. For nonlinear peridynamic models with material failure the localization of zones of softening and damage is the hallmark of peridynamic modeling [Silling, 2000, Silling et al., 2007], [Ha and Bobaru, 2010], [Foster et al., 2011]. One notes that the a-priori error involves  $\epsilon$  in the denominator and in many cases  $\epsilon$  is chosen small. However typical dynamic fracture experiments last only hundreds of microseconds and the a-priori error is controlled by the product of simulation time multiplied by  $h^2 / \epsilon^2$ . So for material properties characteristic of Plexiglass and  $\epsilon$  of size  $4mm$ , the a-priori estimates predict a relative error of 1/10 for simulations lasting around 100 microseconds. We point out that the a-priori error estimates assume the appearance of nonlinearity anywhere in the computational domain. On the other hand numerical simulation and independent theoretical estimates show that the nonlinearity concentrates along “fat” cracks of finite length and width equal to  $\epsilon$ , see [Lipton, 2016, Lipton, 2014]. Moreover the remainder of the computational domain is seen to behave linearly and to leading order can be modeled as a linear elastic material up to

an error proportional to  $\epsilon$ , see [Proposition 6, [Jha and Lipton 2018b]]. Future work will use these observations to focus on adaptive implementation and a-posteriori estimates. A-posteriori convergence for FEM models of peridynamics with material degradation can be seen in the work [Macek and Silling, 2007], [Chen and Gunzburger, 2011], [Ren et al., 2017]. For other nonlinear and nonlocal models adaptive mesh refinement within FE framework for nonlocal models has been explored in [Du et al., 2013c] and convergence of the adaptive FE approximation is rigorously shown. A-posteriori error analysis of linear nonlocal models is carried out in [Du et al., 2013b].

The paper is organized as follows. We introduce the equation of motion in [section 2](#) and present the Lipschitz continuity of the force, existence of peridynamic solution, and the higher temporal regularity necessary for the finite element error analysis. In [section 3](#), we consider the finite element discretization. We prove the stability of a semi-discrete approximation in [subsection 3.1](#). In [section 4](#), we analyze the fully discrete approximation and obtain an a-priori bound on errors. The stability of the fully discrete approximation linearized peridynamic force is shown in [subsection 4.3](#). We present our numerical experiments in [section 5](#). Proofs of the Lipschitz bound on the peridynamic force and higher temporal regularity of solutions is provided in [section 6](#). In [section 7](#) we present our conclusions.

We conclude the introduction by listing the notation used throughout the paper. We denote material domain as  $D$  where  $D \subset \mathbb{R}^d$  for  $d = 2, 3$ . Points and vectors in  $\mathbb{R}^d$  are denoted as bold letters. Some of the key notations are as follows

$[0, T]$	Time domain
$\epsilon$	Size of horizon
$\rho$	Density
$H_\epsilon(\mathbf{x})$	Horizon of $\mathbf{x} \in D$ , a ball of radius $\epsilon$ centered at $\mathbf{x}$
$\omega_d$	Volume of unit ball in dimension $d = 2, 3$
$\omega(\mathbf{x}) \in [0, 1]$	Boundary function defined on $D$ taking value 1 in the interior and smoothly decaying to 0 as $\mathbf{x}$ approaches $\partial D$
$\mathbf{u}$	Displacement field defined over $D \times [0, T]$ . We may also use notation $\mathbf{u}$ to denote field defined over just $D$
$\mathbf{u}_0, \mathbf{v}_0$	Initial condition on displacement
$\mathbf{b}$	Body force defined over $D \times [0, T]$
$\mathbf{e}_{\mathbf{y}-\mathbf{x}}$	The unit vector pointing from a point $\mathbf{y}$ to the point $\mathbf{x}$
$S = S(\mathbf{y}, \mathbf{x}, t; \mathbf{u})$	Bond strain $S = \frac{\mathbf{u}(\mathbf{y}, t) - \mathbf{u}(\mathbf{x}, t)}{ \mathbf{y} - \mathbf{x} } \cdot \mathbf{e}_{\mathbf{y}-\mathbf{x}}$ . We may also use $S(\mathbf{y}, \mathbf{x}; \mathbf{u})$ if $\mathbf{u}$ is a field defined over just $D$
$\theta = \theta(\mathbf{x}, t; \mathbf{u})$	Spherical or hydrostatic strain. We may also use $\theta(\mathbf{x}; \mathbf{u})$ if $\mathbf{u}$ is a field defined over just $D$
$S_c^+, S_c^-$	Critical bond strain
$\theta_c^+, \theta_c^-$	Critical hydrostatic strain
$J^\epsilon(r) = J(r/\epsilon)$	Influence function where $J$ is integrable with $J(r) = 0$ for $r \geq 1$ and $0 \leq J(r) \leq M$ for $r < 1$
$\bar{J}_\alpha$	Moment of function $J$ over $H_1(\mathbf{0})$ with weight $1/(\omega_d  \boldsymbol{\xi} ^\alpha)$
$f, g$	Potential functions for pairwise and state-based interaction
$\mathcal{W}^\epsilon, \mathcal{V}^\epsilon$	Pairwise and state-based potential energy density
$PD^\epsilon(\mathbf{u}(t))$	Total peridynamic potential energy at time $t$
$\mathcal{E}^\epsilon(\mathbf{u})(t)$	Total dynamic energy at time $t$
$\mathcal{L}^\epsilon, \mathcal{L}_T^\epsilon, \mathcal{L}_D^\epsilon$	total peridynamic force, pairwise peridynamic force, and state-based peridynamic force respectively
$a^\epsilon(\mathbf{u}, \mathbf{v})$	Nonlinear operator where $\mathbf{u}, \mathbf{v}$ are vector fields over $D$
$a_T^\epsilon, a_D^\epsilon$	Nonlinear pairwise and state-based operator
$\ \cdot\ , \ \cdot\ _\infty, \ \cdot\ _n$	$L^2$ norm over $D$ , $L^\infty$ norm over $D$ , and Sobolev $H^n$ norm over $D$ (for $n = 1, 2$ ) respectively
$h, \Delta t$	Size of mesh and size of time step
$\mathcal{T}_h$	Triangulation of $D$ given by triangular/tetrahedral elements
$\mathcal{I}_h$	Continuous piecewise linear interpolation operator on $\mathcal{T}_h$
$W$	Space of functions in $H^2(D; \mathbb{R}^d)$ such that trace of function is zero on boundary $\partial D$ , i.e. $W = H^2(D; \mathbb{R}^d) \cap H_0^1(D; \mathbb{R}^d)$
$V_h$	Space of continuous piecewise linear interpolations on $\mathcal{T}_h$
$\phi_i$	Interpolation function of mesh node $i$
$\mathbf{r}_h(\mathbf{u})$	Finite element projection of $\mathbf{u}$ onto $V_h$
$E^k$	Total error in mean square norm at time step $k$
$\mathbf{u}_h^k, \mathbf{v}_h^k$	Approximate displacement and velocity field at time step $k$
$\mathbf{u}^k, \mathbf{v}^k$	Exact displacement and velocity field at time step $k$

**2. Equation of motion, existence, uniqueness, and higher regularity.** We assume  $D$  to be an open set with  $C^1$  boundary. To enforce zero displacement boundary conditions at  $\partial D$  and to insure a well posed evolution we introduce the boundary function  $\omega(\mathbf{x})$ . This function is introduced as a factor into the potentials  $\mathcal{W}^\epsilon$  and  $\mathcal{V}^\epsilon$ . Here the boundary function takes value 1 in the interior of domain and is zero on the boundary. We assume  $\sup_{\mathbf{x}} |\nabla \omega(\mathbf{x})| < \infty$  and  $\sup_{\mathbf{x}} |\nabla^2 \omega(\mathbf{x})| < \infty$  in our analysis. The hydrostatic strain

is modified to include the boundary and is given by

$$(6) \quad \theta(\mathbf{x}, t; \mathbf{u}) = \frac{1}{\epsilon^d \omega_d} \int_{H_\epsilon(\mathbf{x})} \omega(\mathbf{y}) J^\epsilon(|\mathbf{y} - \mathbf{x}|) S(\mathbf{y}, \mathbf{x}, t; \mathbf{u}) |\mathbf{y} - \mathbf{x}| d\mathbf{y}.$$

The peridynamic potentials [Equation 2](#) and [Equation 4](#) are modified to *see the boundary* follows

$$(7) \quad \mathcal{W}^\epsilon(S(\mathbf{y}, \mathbf{x}, t; \mathbf{u})) = \omega(\mathbf{x}) \omega(\mathbf{y}) \frac{J^\epsilon(|\mathbf{y} - \mathbf{x}|)}{\epsilon |\mathbf{y} - \mathbf{x}|} f(\sqrt{|\mathbf{y} - \mathbf{x}|} S(\mathbf{y}, \mathbf{x}, t; \mathbf{u})),$$

$$(8) \quad \mathcal{V}^\epsilon(\theta(\mathbf{x}, t; \mathbf{u})) = \omega(\mathbf{x}) \frac{g(\theta(\mathbf{x}, t; \mathbf{u}))}{\epsilon^2}.$$

We assume that potential function  $f$  is at least 4 times differentiable and satisfies following regularity condition:

$$(9) \quad C_0^f := \sup_r |f(r)| < \infty, \quad C_i^f := \sup_r |f^{(i)}(r)| < \infty, \quad \forall i = 1, 2, 3, 4.$$

If potential function  $g$  is convex-concave type then we assume that  $g$  satisfies same regularity condition as  $f$ . We denote constants  $C_i^g$ , for  $i = 0, 1, \dots, 4$ , similar to  $C_i^f$  above.

The total potential energy at time  $t$  is given by

$$(10) \quad PD^\epsilon(\mathbf{u}(t)) = \frac{1}{\epsilon^d \omega_d} \int_D \int_{H_\epsilon(\mathbf{x})} |\mathbf{y} - \mathbf{x}| \mathcal{W}^\epsilon(S(\mathbf{y}, \mathbf{x}, t; \mathbf{u})) d\mathbf{y} d\mathbf{x} \\ + \int_D \mathcal{V}^\epsilon(\theta(\mathbf{x}, t; \mathbf{u})) d\mathbf{x},$$

where potential  $\mathcal{W}^\epsilon$  and  $\mathcal{V}^\epsilon$  are described above. The material is assumed to be homogeneous and the density is given by  $\rho$ . The applied body force is denoted by  $\mathbf{b}(\mathbf{x}, t)$ . We define the Lagrangian

$$\mathbf{L}(\mathbf{u}, \partial_t \mathbf{u}, t) = \frac{\rho}{2} \|\dot{\mathbf{u}}\|^2 - PD^\epsilon(\mathbf{u}(t)) + \int_D \mathbf{b}(t) \cdot \mathbf{u}(t) d\mathbf{x},$$

here  $\dot{\mathbf{u}}$  is the velocity given by the time derivative of  $\mathbf{u}$ . Applying the principal of least action together with a straight forward calculation (see for example [\[Lipton et al., 2018a\]](#) for detailed derivation) gives the nonlocal dynamics

$$(11) \quad \rho \ddot{\mathbf{u}}(\mathbf{x}, t) = \mathcal{L}^\epsilon(\mathbf{u})(\mathbf{x}, t) + \mathbf{b}(\mathbf{x}, t), \quad \text{for } \mathbf{x} \in D,$$

where

$$(12) \quad \mathcal{L}^\epsilon(\mathbf{u})(\mathbf{x}, t) = \mathcal{L}_T^\epsilon(\mathbf{u})(\mathbf{x}, t) + \mathcal{L}_D^\epsilon(\mathbf{u})(\mathbf{x}, t),$$

$\mathcal{L}_T^\epsilon(\mathbf{u})$  is the peridynamic force due to bond-based interaction and is given by

$$(13) \quad \mathcal{L}_T^\epsilon(\mathbf{u})(\mathbf{x}, t) \\ = \frac{2}{\epsilon^d \omega_d} \int_{H_\epsilon(\mathbf{x})} \omega(\mathbf{x}) \omega(\mathbf{y}) \frac{J^\epsilon(|\mathbf{y} - \mathbf{x}|)}{\epsilon |\mathbf{y} - \mathbf{x}|} \partial_S f(\sqrt{|\mathbf{y} - \mathbf{x}|} S(\mathbf{y}, \mathbf{x}, t; \mathbf{u})) \mathbf{e}_{\mathbf{y} - \mathbf{x}} d\mathbf{y},$$

and  $\mathcal{L}_D^\epsilon(\mathbf{u})$  is the peridynamic force due to state-based interaction and is given by

$$(14) \quad \mathcal{L}_D^\epsilon(\mathbf{u})(\mathbf{x}, t) \\ = \frac{1}{\epsilon^d \omega_d} \int_{H_\epsilon(\mathbf{x})} \omega(\mathbf{x}) \omega(\mathbf{y}) \frac{J^\epsilon(|\mathbf{y} - \mathbf{x}|)}{\epsilon^2} [\partial_\theta g(\theta(\mathbf{y}, t; \mathbf{u})) + \partial_\theta g(\theta(\mathbf{x}, t; \mathbf{u}))] \mathbf{e}_{\mathbf{y} - \mathbf{x}} d\mathbf{y}.$$

The dynamics is complemented with the initial data

$$(15) \quad \mathbf{u}(\mathbf{x}, 0) = \mathbf{u}_0(\mathbf{x}), \quad \partial_t \mathbf{u}(\mathbf{x}, 0) = \mathbf{v}_0(\mathbf{x}).$$

We prescribe zero Dirichlet boundary condition on the boundary  $\partial D$

$$(16) \quad \mathbf{u}(\mathbf{x}) = \mathbf{0} \quad \forall \mathbf{x} \in \partial D.$$

We extend the zero boundary condition outside  $D$  to whole  $\mathbb{R}^d$ . In our analysis we will assume mass density  $\rho = 1$  without loss of generality.

**2.1. Existence of solutions and higher regularity in time.** We recall that the space  $H_0^n(D; \mathbb{R}^d)$  is the closure in the  $H^n$  norm of the functions that are infinitely differentiable with compact support in  $D$ . For suitable initial conditions and body force we show that solutions exist in

$$(17) \quad W = H^2(D; \mathbb{R}^d) \cap H_0^1(D; \mathbb{R}^d) = \{v \in H^2(D; \mathbb{R}^d) : \gamma v = 0, \text{ on } \partial D\}$$

where  $\gamma$  is the trace of the function  $v$  on the boundary of  $D$ . We will assume that  $\mathbf{u} \in W$  is extended by zero outside  $D$ . We first exhibit the Lipschitz continuity property and boundedness of the peridynamic force for displacements in  $W$ . We will then apply [Theorem 3.2, [Jha and Lipton, 2017]] to conclude the existence of unique solutions.

We note the following Sobolev embedding properties of  $H^2(D; \mathbb{R}^d)$  when  $D$  is a  $C^1$  domain.

- From Theorem 2.72 of [Demengel, 2012], there exists a constant  $C_{e_1}$  independent of  $\mathbf{u} \in H^2(D; \mathbb{R}^d)$  such that

$$(18) \quad \|\mathbf{u}\|_\infty \leq C_{e_1} \|\mathbf{u}\|_2.$$

- Further application of standard embedding theorems (e.g., Theorem 2.72 of [Demengel, 2012]), shows there exists a constant  $C_{e_2}$  independent of  $\mathbf{u}$  such that

$$(19) \quad \|\nabla \mathbf{u}\|_{L^q(D; \mathbb{R}^{d \times d})} \leq C_{e_2} \|\nabla \mathbf{u}\|_1 \leq C_{e_2} \|\mathbf{u}\|_2,$$

for any  $q$  such that  $2 \leq q < \infty$  when  $d = 2$  and  $2 \leq q \leq 6$  when  $d = 3$ .

We have following result which show the Lipschitz continuity property of a peridynamic force  $\mathcal{L}^\epsilon$ .

**THEOREM 1. Lipschitz continuity of peridynamic force**

Let  $f$  be a convex-concave function satisfying  $C_i^f < \infty$  for  $i = 0, \dots, 4$  and let  $g$  either be a quadratic function, or  $g$  be a convex-concave function with  $C_i^g < \infty$  for  $i = 0, \dots, 4$ . Also, let boundary function  $\omega : D \rightarrow [0, 1]$  be such that  $\sup_{\mathbf{x} \in D} |\nabla \omega(\mathbf{x})| < \infty$  and  $\sup_{\mathbf{x} \in D} |\nabla^2 \omega(\mathbf{x})| < \infty$ . Then, for any  $\mathbf{u}, \mathbf{v} \in W$ , we have

$$(20) \quad \|\mathcal{L}^\epsilon(\mathbf{u}) - \mathcal{L}^\epsilon(\mathbf{v})\|_2 \leq \frac{\bar{L}_1(1 + \|\mathbf{u}\|_2 + \|\mathbf{v}\|_2)^2}{\epsilon^3} \|\mathbf{u} - \mathbf{v}\|_2,$$

where constant  $\bar{L}_1$  does not depend on  $\epsilon$  and  $\mathbf{u}, \mathbf{v}$ . Also, for  $\mathbf{u} \in W$ , we have

$$(21) \quad \|\mathcal{L}^\epsilon(\mathbf{u})\|_2 \leq \frac{\bar{L}_2(\|\mathbf{u}\|_2 + \|\mathbf{u}\|_2^2)}{\epsilon^{5/2}},$$

where constant  $\bar{L}_2$  does not depend on  $\epsilon$  and  $\mathbf{u}$ .



Now let  $T > 0$  be any positive number, a straight-forward application of [Theorem 3.2, [Jha and Lipton, 2017]] gives:

**THEOREM 2. *Existence and uniqueness of solutions over finite time intervals***  
 Let  $f$ ,  $g$ , and  $\omega$  satisfy the hypothesis of [Theorem 1](#). For any initial condition  $\mathbf{u}_0, \mathbf{v}_0 \in W$ , time interval  $I_0 = (-T, T)$ , and right hand side  $\mathbf{b}(t)$  continuous in time for  $t \in I_0$  such that  $\mathbf{b}(t)$  satisfies  $\sup_{t \in I_0} \|\mathbf{b}(t)\|_2 < \infty$ , there is a unique solution  $\mathbf{u}(t) \in C^2(I_0; W)$  of peridynamic equation [11](#). Also,  $\mathbf{u}(t)$  and  $\dot{\mathbf{u}}(t)$  are Lipschitz continuous in time for  $t \in I_0$ .

We can also show higher regularity in time of evolutions under suitable assumptions on the body force:

**THEOREM 3. *Higher regularity***  
 Suppose the initial data and righthand side  $\mathbf{b}(t)$  satisfy the hypothesis of [Theorem 2](#) and suppose further that  $\dot{\mathbf{b}}(t)$  exists and is continuous in time for  $t \in I_0$  and  $\sup_{t \in I_0} \|\dot{\mathbf{b}}(t)\|_2 < \infty$ . Then  $\mathbf{u} \in C^3(I_0; W)$  and

$$(22) \quad \|\partial_{ttt}^3 \mathbf{u}(\mathbf{x}, t)\|_2 \leq \frac{C(1 + \sup_{s \in I_0} \|\mathbf{u}(s)\|_2)^2}{\epsilon^3} \sup_{s \in I_0} \|\partial_t \mathbf{u}(s)\|_2 + \|\dot{\mathbf{b}}(\mathbf{x}, t)\|_2,$$

where  $C$  is a positive constant independent of  $\mathbf{u}$ .

The proofs of [Theorems 1](#), and [3](#) are given in [section 6](#). For future reference, we note that for any  $\mathbf{u}, \mathbf{v} \in L_0^2(D; \mathbb{R}^d)$ , we have

$$(23) \quad \|\mathcal{L}^\epsilon(\mathbf{u}) - \mathcal{L}^\epsilon(\mathbf{v})\| \leq \frac{L}{\epsilon^2} \|\mathbf{u} - \mathbf{v}\|.$$

where constant  $L$  is given by

$$(24) \quad L := \begin{cases} 4(C_2^f \bar{J}_1 + C_2^g \bar{J}_0^2) & \text{if } g \text{ is a convex-concave type,} \\ 4(C_2^f \bar{J}_1 + g''(0) \bar{J}_0^2) & \text{if } g \text{ is a quadratic function,} \end{cases}$$

and  $\bar{J}^\alpha = (1/\omega_d) \int_{H_1(\mathbf{0})} J(|\boldsymbol{\xi}|)/|\boldsymbol{\xi}|^\alpha d\boldsymbol{\xi}$ .

**2.2. Weak form.** We multiply [Equation 11](#) by a test function  $\tilde{\mathbf{u}}$  in  $H_0^1(D; \mathbb{R}^d)$  and integrate over  $D$  to get

$$(25) \quad (\ddot{\mathbf{u}}(t), \tilde{\mathbf{u}}) = (\mathcal{L}^\epsilon(\mathbf{u}(t)), \tilde{\mathbf{u}}) + (\mathbf{b}(t), \tilde{\mathbf{u}}).$$

We have the following integration by parts formula:

**LEMMA 4.** For any  $\mathbf{u}, \mathbf{v} \in L_0^2(D; \mathbb{R}^d)$  we have

$$(26) \quad (\mathcal{L}^\epsilon(\mathbf{u}), \mathbf{v}) = -a^\epsilon(\mathbf{u}, \mathbf{v}),$$

where

$$(27) \quad a^\epsilon(\mathbf{u}, \mathbf{v}) = a_T^\epsilon(\mathbf{u}, \mathbf{v}) + a_D^\epsilon(\mathbf{u}, \mathbf{v})$$

and

$$(28) \quad \begin{aligned} a_T^\epsilon(\mathbf{u}, \mathbf{v}) &= \frac{1}{\epsilon^{d+1} \omega_d} \int_D \int_D \omega(\mathbf{x}) \omega(\mathbf{y}) J^\epsilon(|\mathbf{y} - \mathbf{x}|) \\ &\quad \partial_S f(\sqrt{|\mathbf{y} - \mathbf{x}|} S(\mathbf{y}, \mathbf{x}; \mathbf{u})) S(\mathbf{y}, \mathbf{x}; \mathbf{v}) d\mathbf{y} d\mathbf{x}, \\ a_D^\epsilon(\mathbf{u}, \mathbf{v}) &= \frac{1}{\epsilon^2} \int_D \omega(\mathbf{x}) g'(\theta(\mathbf{x}; \mathbf{u})) \theta(\mathbf{x}; \mathbf{v}) d\mathbf{x}. \end{aligned}$$

The proof of above lemma is identical to the proof of Lemma 4.2 in [Lipton et al., 2018a].

Using the above Lemma, the weak form of the peridynamic evolution is given by

$$(29) \quad (\ddot{\mathbf{u}}(t), \tilde{\mathbf{u}}) + a^\epsilon(\mathbf{u}(t), \tilde{\mathbf{u}}) = (\mathbf{b}(t), \tilde{\mathbf{u}}).$$

*Total dynamic energy:* We define the total dynamic energy as follows

$$(30) \quad \mathcal{E}^\epsilon(\mathbf{u})(t) = \frac{1}{2} \|\dot{\mathbf{u}}(t)\|_{L^2}^2 + PD^\epsilon(\mathbf{u}(t)),$$

where  $PD^\epsilon$  is defined in Equation 10. Time derivative of total energy satisfies

$$(31) \quad \frac{d}{dt} \mathcal{E}^\epsilon(\mathbf{u})(t) = (\ddot{\mathbf{u}}(t), \dot{\mathbf{u}}(t)) + a^\epsilon(\mathbf{u}(t), \dot{\mathbf{u}}(t)).$$

**Remark.** It is readily verified that the peridynamic force and energy are bounded for all functions in  $L^2(D; \mathbb{R}^d)$ . Here the bound on the force follows from the Lipschitz property of the force in  $L^2(D; \mathbb{R}^d)$ , see, Equation 23. The peridynamic force is also bounded for functions  $\mathbf{u}$  in  $H^1(D; \mathbb{R}^d)$ . This again follows from the Lipschitz property of the force in  $H^1(D; \mathbb{R}^d)$  using arguments established in section 6. The boundedness of the energy  $PD^\epsilon(\mathbf{u})$  in both  $L^2(D; \mathbb{R}^d)$  and  $H^1(D; \mathbb{R}^d)$  follows from the boundedness of the bond potential energy  $\mathcal{W}^\epsilon(S(\mathbf{y}, \mathbf{x}, t; \mathbf{u}))$  and  $\mathcal{V}^\epsilon(\theta(\mathbf{x}, t; \mathbf{u}))$  used in the definition of  $PD^\epsilon(\mathbf{u})$ , see Equation 7 and Equation 8. More generally this also shows that  $PD^\epsilon(\mathbf{u}) < \infty$  for  $\mathbf{u} \in L^1(D; \mathbb{R}^d)$ .

We next discuss the spatial and the time discretization of peridynamic equation.

**3. Finite element approximation.** Let  $V_h$  be given by linear continuous interpolations over tetrahedral or triangular elements  $\mathcal{T}_h$  where  $h$  denotes the size of finite element mesh. Here we assume the elements are conforming and the finite element mesh is shape regular and  $V_h \subset H_0^1(D; \mathbb{R}^d)$ .

For a continuous function  $\mathbf{u}$  on  $\bar{D}$ ,  $\mathcal{I}_h(\mathbf{u})$  is the continuous piecewise linear interpolant on  $\mathcal{T}_h$ . It is given by

$$(32) \quad \mathcal{I}_h(\mathbf{u}) \Big|_T = \mathcal{I}_T(\mathbf{u}) \quad \forall T \in \mathcal{T}_h,$$

where  $\mathcal{I}_T(\mathbf{u})$  is the local interpolant defined over finite element  $T$  and is given by

$$(33) \quad \mathcal{I}_T(\mathbf{u}) = \sum_{i=1}^n \mathbf{u}(\mathbf{x}_i) \phi_i.$$

Here  $n$  is the number of vertices in an element  $T$ ,  $\mathbf{x}_i$  is the position of vertex  $i$ , and  $\phi_i$  is the linear interpolant associated to vertex  $i$ .

Application of Theorem 4.4.20 and remark 4.4.27 in [Brenner and Scott, 2007] gives

$$(34) \quad \|\mathbf{u} - \mathcal{I}_h(\mathbf{u})\| \leq ch^2 \|\mathbf{u}\|_2, \quad \forall \mathbf{u} \in W.$$

Let  $\mathbf{r}_h(\mathbf{u})$  denote the projection of  $\mathbf{u} \in W$  on  $V_h$ . For the  $L^2$  norm it is defined as

$$(35) \quad \|\mathbf{u} - \mathbf{r}_h(\mathbf{u})\| = \inf_{\tilde{\mathbf{u}} \in V_h} \|\mathbf{u} - \tilde{\mathbf{u}}\|.$$

and satisfies

$$(36) \quad (\mathbf{r}_h(\mathbf{u}), \tilde{\mathbf{u}}) = (\mathbf{u}, \tilde{\mathbf{u}}), \quad \forall \tilde{\mathbf{u}} \in V_h.$$

Since  $\mathcal{I}_h(\mathbf{u}) \in V_h$ , and Equation 34 we see that

$$(37) \quad \|\mathbf{u} - \mathbf{r}_h(\mathbf{u})\| \leq ch^2 \|\mathbf{u}\|_2, \quad \forall \mathbf{u} \in W$$

**3.1. Semi-discrete approximation.** Let  $\mathbf{u}_h(t) \in V_h$  be the approximation of  $\mathbf{u}(t)$  satisfying following for all  $t \in [0, T]$

$$(38) \quad (\dot{\mathbf{u}}_h, \tilde{\mathbf{u}}) + a^\epsilon(\mathbf{u}_h(t), \tilde{\mathbf{u}}) = (\mathbf{b}(t), \tilde{\mathbf{u}}), \quad \forall \tilde{\mathbf{u}} \in V_h.$$

We have following result:

**THEOREM 5. Energy stability of semi-discrete approximation**

The semi-discrete scheme is stable and the energy  $\mathcal{E}^\epsilon(\mathbf{u}_h)(t)$ , defined in Equation 30, satisfies the following bound

$$\mathcal{E}^\epsilon(\mathbf{u}_h)(t) \leq \left[ \sqrt{\mathcal{E}^\epsilon(\mathbf{u}_h)(0)} + \int_0^t \|\mathbf{b}(\tau)\| d\tau \right]^2.$$

We note that while proving the stability of semi-discrete scheme corresponding to nonlinear peridynamics, we do not require any assumption on the strain  $S(\mathbf{y}, \mathbf{x}, t; \mathbf{u}_h)$ . The proof is similar to [Section 6.2, [Lipton, 2016]].

*Proof.* Letting  $\tilde{\mathbf{u}} = \dot{\mathbf{u}}_h(t)$  in Equation 38 and noting the identity Equation 31, we get

$$(39) \quad \frac{d}{dt} \mathcal{E}^\epsilon(\mathbf{u}_h)(t) = (\mathbf{b}(t), \dot{\mathbf{u}}_h(t)) \leq \|\mathbf{b}(t)\| \|\dot{\mathbf{u}}_h(t)\|.$$

We also have

$$\|\dot{\mathbf{u}}_h(t)\| \leq 2\sqrt{\frac{1}{2}\|\dot{\mathbf{u}}_h\|^2 + PD^\epsilon(\mathbf{u}_h(t))} = 2\sqrt{\mathcal{E}^\epsilon(\mathbf{u}_h)(t)}$$

where we used the fact that  $PD^\epsilon(\mathbf{u})(t)$  is nonnegative. We substitute above inequality in Equation 39 to get

$$\frac{d}{dt} \mathcal{E}^\epsilon(\mathbf{u}_h)(t) \leq 2\sqrt{\mathcal{E}^\epsilon(\mathbf{u}_h)(t)} \|\mathbf{b}(t)\|.$$

We fix  $\delta > 0$  and define  $A(t)$  as  $A(t) = \mathcal{E}^\epsilon(\mathbf{u}_h)(t) + \delta$ . Then, from the above equation we easily have

$$\frac{d}{dt} A(t) \leq 2\sqrt{A(t)} \|\mathbf{b}(t)\| \quad \Rightarrow \quad \frac{1}{2} \frac{\frac{d}{dt} A(t)}{\sqrt{A(t)}} \leq \|\mathbf{b}(t)\|.$$

Noting that  $\frac{1}{\sqrt{a(t)}} \frac{da(t)}{dt} = 2 \frac{d}{dt} \sqrt{a(t)}$ , integrating from  $t = 0$  to  $\tau$  and relabeling  $\tau$  as  $t$ , we get

$$\sqrt{A(t)} \leq \sqrt{A(0)} + \int_0^t \|\mathbf{b}(s)\| ds.$$

Proof is complete once we let  $\delta \rightarrow 0$  and take the square of both sides.  $\square$

**4. Central difference time discretization.** In subsection 4.2 we calculate the convergence rate for the central difference time discretization of the fully nonlinear problem. We then present a CFL like condition on the time step  $\Delta t$  for the linearized peridynamic equation in subsection 4.3.

At time step  $k$ , the exact solution is given by  $(\mathbf{u}^k, \mathbf{v}^k)$  where  $\mathbf{v}^k = \partial \mathbf{u}^k / \partial t$ , and their projection onto  $V_h$  is given by  $(\mathbf{r}_h(\mathbf{u}^k), \mathbf{r}_h(\mathbf{v}^k))$ . The solution of fully discrete problem at time step  $k$  is given by  $(\mathbf{u}_h^k, \mathbf{v}_h^k)$ .

We approximate the initial data on displacement  $\mathbf{u}_0$  and velocity  $\mathbf{v}_0$  by their projections  $\mathbf{r}_h(\mathbf{u}_0)$  and  $\mathbf{r}_h(\mathbf{v}_0)$ . Let  $\mathbf{u}_h^0 = \mathbf{r}_h(\mathbf{u}_0)$  and  $\mathbf{v}_h^0 = \mathbf{r}_h(\mathbf{v}_0)$ . For  $k \geq 1$ ,  $(\mathbf{u}_h^k, \mathbf{v}_h^k)$  satisfies, for all  $\tilde{\mathbf{u}} \in V_h$ ,

$$(40) \quad \begin{aligned} \left( \frac{\mathbf{u}_h^{k+1} - \mathbf{u}_h^k}{\Delta t}, \tilde{\mathbf{u}} \right) &= (\mathbf{v}_h^{k+1}, \tilde{\mathbf{u}}), \\ \left( \frac{\mathbf{v}_h^{k+1} - \mathbf{v}_h^k}{\Delta t}, \tilde{\mathbf{u}} \right) &= (\mathcal{L}^\epsilon(\mathbf{u}_h^k), \tilde{\mathbf{u}}) + (\mathbf{b}_h^k, \tilde{\mathbf{u}}), \end{aligned}$$

where we have denoted the projection of  $\mathbf{b}(t^k)$ , i.e.  $\mathbf{r}_h(\mathbf{b}(t^k))$ , as  $\mathbf{b}_h^k$ . Combining the two equations delivers central difference equation for  $\mathbf{u}_h^k$ . We have

$$(41) \quad \left( \frac{\mathbf{u}_h^{k+1} - 2\mathbf{u}_h^k + \mathbf{u}_h^{k-1}}{\Delta t^2}, \tilde{\mathbf{u}} \right) = (\mathcal{L}^\epsilon(\mathbf{u}_h^k), \tilde{\mathbf{u}}) + (\mathbf{b}_h^k, \tilde{\mathbf{u}}), \quad \forall \tilde{\mathbf{u}} \in V_h.$$

For  $k = 0$ , we have  $\forall \tilde{\mathbf{u}} \in V_h$

$$(42) \quad \left( \frac{\mathbf{u}_h^1 - \mathbf{u}_h^0}{\Delta t^2}, \tilde{\mathbf{u}} \right) = \frac{1}{2}(\mathcal{L}^\epsilon(\mathbf{u}_h^0), \tilde{\mathbf{u}}) + \frac{1}{\Delta t}(\mathbf{v}_h^0, \tilde{\mathbf{u}}) + \frac{1}{2}(\mathbf{b}_h^0, \tilde{\mathbf{u}}).$$

**4.1. Implementation details.** For completeness we describe the implementation of the time stepping method using FEM interpolants. Let  $\mathbf{N}$  be the shape tensor then  $\mathbf{u}_h^k, \tilde{\mathbf{u}} \in V_h$  are given by

$$(43) \quad \mathbf{u}_h^k = \mathbf{N}\mathbf{U}^k, \quad \tilde{\mathbf{u}} = \mathbf{N}\tilde{\mathbf{U}},$$

where  $\mathbf{U}^k$  and  $\tilde{\mathbf{U}}$  are  $Nd$  dimensional vectors, where  $N$  is the number of nodal points in the mesh and  $d$  is the dimension.

From Equation 41, for all  $\tilde{\mathbf{U}} \in \mathbb{R}^{Nd}$  with elements of  $\tilde{\mathbf{U}}$  zero on the boundary, then the following holds for  $k \geq 1$

$$(44) \quad \left[ \mathbf{M} \frac{\mathbf{U}^{k+1} - 2\mathbf{U}^k + \mathbf{U}^{k-1}}{\Delta t^2} \right] \cdot \tilde{\mathbf{U}} = \mathbf{F}^k \cdot \tilde{\mathbf{U}}.$$

Here the mass matrix  $\mathbf{M}$  and force vector  $\mathbf{F}^k$  are given by

$$(45) \quad \begin{aligned} \mathbf{M} &:= \int_D \mathbf{N}^T \mathbf{N} d\mathbf{x}, \\ \mathbf{F}^k &:= \mathbf{F}_{pd}^k + \int_D \mathbf{N}^T \mathbf{b}(\mathbf{x}, t^k) d\mathbf{x}, \end{aligned}$$

where  $\mathbf{F}_{pd}^k$  is defined by

$$(46) \quad \mathbf{F}_{pd}^k := \int_D \mathbf{N}^T (\mathcal{L}^\epsilon(\mathbf{u}_h^k)(\mathbf{x})) d\mathbf{x}.$$

We remark that a similar equation holds for  $k = 0$ .

At the time step  $k$  we must invert  $\mathbf{M}$  to solve for  $\mathbf{U}^{k+1}$  using

$$(47) \quad \mathbf{U}^{k+1} = \Delta t^2 \mathbf{M}^{-1} \mathbf{F}^k + 2\mathbf{U}^k - \mathbf{U}^{k-1}.$$

As is well known this inversion amounts to an increase of computational complexity associated with discrete approximation of the weak formulation of the evolution. Further, the matrix-vector multiplication  $\mathbf{M}^{-1}\mathbf{F}^k$  needs to be carried out at each time step. On the other hand the quadrature error in the computation of the force vector  $\mathbf{F}_{pd}^k$  is reduced when using the weak form.

We next show the convergence of approximation.

**4.2. Convergence of approximation.** In this section, we prove the uniform bound on the error and show that the approximate solution converges to the exact solution with rate given by  $C_t\Delta t + C_s h^2/\epsilon^2$ . Here horizon  $\epsilon > 0$  is assumed to be fixed. We first compare the exact solution with its projection in  $V_h$  and then compare the projection with the approximate solution. We further divide the calculation of error between the projection and the approximate solution in two parts, namely consistency analysis and error analysis.

Error  $E^k$  is given by

$$E^k := \|\mathbf{u}_h^k - \mathbf{u}(t^k)\| + \|\mathbf{v}_h^k - \mathbf{v}(t^k)\|.$$

The error is split into two parts as follows

$$E^k \leq (\|\mathbf{u}^k - \mathbf{r}_h(\mathbf{u}^k)\| + \|\mathbf{v}^k - \mathbf{r}_h(\mathbf{v}^k)\|) + (\|\mathbf{r}_h(\mathbf{u}^k) - \mathbf{u}_h^k\| + \|\mathbf{r}_h(\mathbf{v}^k) - \mathbf{v}_h^k\|),$$

where the first term is the error between the exact solution and projection, and the second term is the error between the projection and approximate solution. Let

$$(48) \quad \mathbf{e}_h^k(\mathbf{u}) := \mathbf{r}_h(\mathbf{u}^k) - \mathbf{u}_h^k \quad \text{and} \quad \mathbf{e}_h^k(\mathbf{v}) := \mathbf{r}_h(\mathbf{v}^k) - \mathbf{v}_h^k$$

and

$$(49) \quad e^k := \|\mathbf{e}_h^k(\mathbf{u})\| + \|\mathbf{e}_h^k(\mathbf{v})\|.$$

Using Equation 37, we have

$$(50) \quad E^k \leq C_p h^2 + e^k,$$

where

$$(51) \quad C_p := c \left[ \sup_t \|\mathbf{u}(t)\|_2 + \sup_t \left\| \frac{\partial \mathbf{u}(t)}{\partial t} \right\|_2 \right].$$

We have the following a-priori convergence rate given by

**THEOREM 6. Convergence of Central difference approximation**

Let  $(\mathbf{u}, \mathbf{v})$  be the exact solution of the peridynamic equation 11. Let  $(\mathbf{u}_h^k, \mathbf{v}_h^k)$  be the FE solution of Equation 40. If  $\mathbf{u}, \mathbf{v} \in C^2([0, T]; W)$ , then the scheme is consistent and the error  $E^k$  satisfies following bound

$$(52) \quad \sup_{k \leq T/\Delta t} E^k = C_p h^2 + \exp[T(1 + L/\epsilon^2)(\frac{1}{1 - \Delta t})] \left[ e^0 + \left( \frac{T}{1 - \Delta t} \right) \left( C_t \Delta t + C_s \frac{h^2}{\epsilon^2} \right) \right]$$

where the constants  $C_p$ ,  $C_t$ , and  $C_s$  are given by Equation 51 and Equation 58. The constant  $L/\epsilon^2$  is the Lipschitz constant of the peridynamic force  $\mathcal{L}^\epsilon(\mathbf{u})$  in  $L^2$ , see Equation 23. If the error in initial data is zero then  $E^k$  is of the order of  $C_t \Delta t + C_s h^2/\epsilon^2$ .

In [Theorem 3](#) we have shown that  $\mathbf{u}, \mathbf{v} \in C^2([0, T]; W)$  for righthand side  $\mathbf{b} \in C^1([0, T]; W)$ . In [section 7](#) we discuss the behavior of the exponential constant appearing in [Theorem 6](#) for evolution times seen in fracture experiments. Since we are approximating the solution of an ODE on a Banach space the proof of [Theorem 6](#) will follow from the Lipschitz continuity of the force  $\mathcal{L}^\epsilon(\mathbf{u})$  with respect to the  $L^2$  norm. The proof is given in the following two sections.

**4.2.1. Truncation error analysis and consistency.** The results in this section follows the same steps as in [[Jha and Lipton, 2017](#)] and therefore we will just highlight the major steps. We can write the discrete evolution equation for  $(\mathbf{e}_h^k(\mathbf{u}) = \mathbf{r}_h(\mathbf{u}^k) - \mathbf{u}_h^k, \mathbf{e}_h^k(\mathbf{v}) = \mathbf{r}_h(\mathbf{v}^k) - \mathbf{v}_h^k)$  as follows

$$\begin{aligned} (\mathbf{e}_h^{k+1}(\mathbf{u}), \tilde{\mathbf{u}}) &= (\mathbf{e}_h^k(\mathbf{u}), \tilde{\mathbf{u}}) + \Delta t(\mathbf{e}_h^{k+1}(\mathbf{v}), \tilde{\mathbf{u}}) + \Delta t(\boldsymbol{\tau}_h^k(\mathbf{u}), \tilde{\mathbf{u}}), \\ (\mathbf{e}_h^{k+1}(\mathbf{v}), \tilde{\mathbf{u}}) &= (\mathbf{e}_h^k(\mathbf{v}), \tilde{\mathbf{u}}) + \Delta t(\mathcal{L}^\epsilon(\mathbf{u}_h^k) - \mathcal{L}^\epsilon(\mathbf{r}_h(\mathbf{u}^k)), \tilde{\mathbf{u}}) \\ &\quad + \Delta t(\boldsymbol{\tau}_h^k(\mathbf{v}), \tilde{\mathbf{u}}) + \Delta t(\boldsymbol{\sigma}_h^k(\mathbf{u}), \tilde{\mathbf{u}}), \end{aligned} \tag{53}$$

where consistency error terms  $\boldsymbol{\tau}_h^k(\mathbf{u}), \boldsymbol{\tau}_h^k(\mathbf{v}), \boldsymbol{\sigma}_h^k(\mathbf{u})$  are given by

$$\begin{aligned} \boldsymbol{\tau}_h^k(\mathbf{u}) &:= \frac{\partial \mathbf{u}^{k+1}}{\partial t} - \frac{\mathbf{u}^{k+1} - \mathbf{u}^k}{\Delta t}, \\ \boldsymbol{\tau}_h^k(\mathbf{v}) &:= \frac{\partial \mathbf{v}^k}{\partial t} - \frac{\mathbf{v}^{k+1} - \mathbf{v}^k}{\Delta t}, \\ \boldsymbol{\sigma}_h^k(\mathbf{u}) &:= \mathcal{L}^\epsilon(\mathbf{r}_h(\mathbf{u}^k)) - \mathcal{L}^\epsilon(\mathbf{u}^k). \end{aligned} \tag{54}$$

When  $\mathbf{u}, \mathbf{v}$  are  $C^2$  in time, we easily see that

$$\|\boldsymbol{\tau}_h^k(\mathbf{u})\| \leq \Delta t \sup_t \left\| \frac{\partial^2 \mathbf{u}}{\partial t^2} \right\| \quad \text{and} \quad \|\boldsymbol{\tau}_h^k(\mathbf{v})\| \leq \Delta t \sup_t \left\| \frac{\partial^2 \mathbf{v}}{\partial t^2} \right\|.$$

To estimate  $\boldsymbol{\sigma}_h^k(\mathbf{u})$ , we recall the Lipschitz continuity property of the peridynamic force in the  $L^2$  norm, see [Equation 23](#). This leads us to

$$\|\boldsymbol{\sigma}_h^k(\mathbf{u})\| \leq \frac{L}{\epsilon^2} \|\mathbf{u}^k - \mathbf{r}_h(\mathbf{u}^k)\| \leq \frac{Lc}{\epsilon^2} h^2 \sup_t \|\mathbf{u}(t)\|_2, \tag{55}$$

where the constant  $L$  is defined in [Equation 24](#).

We now state the consistency of this approach.

**LEMMA 7. Consistency**

Let  $\tau$  be given by

$$\tau := \sup_k (\|\boldsymbol{\tau}_h^k(\mathbf{u})\| + \|\boldsymbol{\tau}_h^k(\mathbf{v})\| + \|\boldsymbol{\sigma}_h^k(\mathbf{u})\|), \tag{56}$$

then the approach is consistent in that

$$\tau \leq C_t \Delta t + C_s \frac{h^2}{\epsilon^2}, \tag{57}$$

where

$$C_t := \left\| \frac{\partial^2 \mathbf{u}}{\partial t^2} \right\| + \left\| \frac{\partial^2 \mathbf{v}}{\partial t^2} \right\| \quad \text{and} \quad C_s := Lc \sup_t \|\mathbf{u}(t)\|_2. \tag{58}$$

**4.2.2. Stability analysis.** In equation for  $e_h^k(\mathbf{u})$ , we take  $\tilde{\mathbf{u}} = e_h^{k+1}(\mathbf{u})$ . We have

$$\|e_h^{k+1}(\mathbf{u})\|^2 = (e_h^k(\mathbf{u}), e_h^{k+1}(\mathbf{u})) + \Delta t (e_h^{k+1}(\mathbf{v}), e_h^{k+1}(\mathbf{u})) + \Delta t (\boldsymbol{\tau}_h^k(\mathbf{u}), e_h^{k+1}(\mathbf{u})),$$

which implies

$$(59) \quad \|e_h^{k+1}(\mathbf{u})\| \leq \|e_h^k(\mathbf{u})\| + \Delta t \|e_h^{k+1}(\mathbf{v})\| + \Delta t \|\boldsymbol{\tau}_h^k(\mathbf{u})\|.$$

Similarly, we can show

$$(60) \quad \begin{aligned} \|e_h^{k+1}(\mathbf{v})\| &\leq \|e_h^k(\mathbf{v})\| + \Delta t \|\mathcal{L}^\epsilon(\mathbf{u}_h^k) - \mathcal{L}^\epsilon(\mathbf{r}_h(\mathbf{u}^k))\| \\ &\quad + \Delta t (\|\boldsymbol{\tau}_h^k(\mathbf{v})\| + \|\boldsymbol{\sigma}_{per,h}^k(\mathbf{u})\|). \end{aligned}$$

We have from Equation 23

$$(61) \quad \|\mathcal{L}^\epsilon(\mathbf{u}_h^k) - \mathcal{L}^\epsilon(\mathbf{r}_h(\mathbf{u}^k))\| \leq \frac{L}{\epsilon^2} \|\mathbf{u}_h^k - \mathbf{r}_h(\mathbf{u}^k)\| = \frac{L}{\epsilon^2} \|e_h^k(\mathbf{u})\|.$$

After adding Equation 59 and Equation 60, and substituting Equation 61, we get

$$\|e_h^{k+1}(\mathbf{u})\| + \|e_h^{k+1}(\mathbf{v})\| \leq \|e_h^k(\mathbf{u})\| + \|e_h^k(\mathbf{v})\| + \Delta t \|e_h^{k+1}(\mathbf{v})\| + \frac{L}{\epsilon^2} \Delta t \|e_h^k(\mathbf{u})\| + \Delta t \tau$$

where  $\tau$  is defined in Equation 56. Since  $e^k = \|e_h^k(\mathbf{u})\| + \|e_h^k(\mathbf{v})\|$ , we can show, assuming  $L/\epsilon^2 \geq 1$ ,

$$\begin{aligned} e^{k+1} &\leq e^k + \Delta t e^{k+1} + \Delta t \frac{L}{\epsilon^2} e^k + \Delta t \tau \\ \Rightarrow e^{k+1} &\leq \frac{1 + \Delta t L/\epsilon^2}{1 - \Delta t} e^k + \frac{\Delta t}{1 - \Delta t} \tau. \end{aligned}$$

Substituting for  $e^k$  recursively in the equation above, we get

$$e^{k+1} \leq \left( \frac{1 + \Delta t L/\epsilon^2}{1 - \Delta t} \right)^{k+1} e^0 + \frac{\Delta t}{1 - \Delta t} \tau \sum_{j=0}^k \left( \frac{1 + \Delta t L/\epsilon^2}{1 - \Delta t} \right)^{k-j}.$$

Noting that

$$\frac{1 + \Delta t L/\epsilon^2}{1 - \Delta t} = 1 + \frac{(1 + L/\epsilon^2)}{1 - \Delta t} \Delta t$$

and  $(1 + a\Delta t)^k \leq \exp[ka\Delta t] \leq \exp[Ta]$  for  $a > 0$ , we have

$$(62) \quad \left( \frac{1 + \Delta t L/\epsilon^2}{1 - \Delta t} \right)^k \leq \exp\left[ \frac{T(1 + L/\epsilon^2)}{1 - \Delta t} \right].$$

This implies

$$\begin{aligned} e^{k+1} &\leq \exp\left[ \frac{T(1 + L/\epsilon^2)}{1 - \Delta t} \right] \left[ e^0 + \frac{\Delta t}{1 - \Delta t} \tau \sum_{j=0}^k 1 \right] \\ &\leq \exp\left[ \frac{T(1 + L/\epsilon^2)}{1 - \Delta t} \right] \left[ e^0 + \frac{k\Delta t}{1 - \Delta t} \tau \right]. \end{aligned}$$

By substituting above equation in Equation 50, we get stability of the scheme:

LEMMA 8. **Stability**

$$(63) \quad E^k \leq C_p h^2 + \exp\left[\frac{T(1+L/\epsilon^2)}{1-\Delta t}\right] \left[ e^0 + \frac{k\Delta t}{1-\Delta t} \tau \right].$$

After taking sup over  $k \leq T/\Delta t$  and substituting the bound on  $\tau$  from Lemma 7, we get the desired result and proof of Theorem 6 is complete.

We now consider a stronger notion of stability for the linearized peridynamics model.

**4.3. Linearized peridynamics and energy stability.** In this section, we linearize the peridynamics model and obtain a CFL like stability condition. For problems where strains are small, the stability condition for the linearized model is expected to apply to the nonlinear model. The slope of peridynamics potential  $f$  and  $g$  are constant for sufficiently small strain and therefore for small strain the nonlinear model behaves like a linear model.

In Equation 13, linearization gives

$$(64) \quad \mathcal{L}_{T,l}^\epsilon(\mathbf{u})(\mathbf{x}) = \frac{2}{\epsilon^{d+1}\omega_d} \int_{H_\epsilon(\mathbf{x})} \omega(\mathbf{x})\omega(\mathbf{y})J^\epsilon(|\mathbf{y}-\mathbf{x}|)f''(0)S(\mathbf{y},\mathbf{x};\mathbf{u})\mathbf{e}_{\mathbf{y}-\mathbf{x}}d\mathbf{y}.$$

The corresponding bilinear form is denoted as  $a_{T,l}^\epsilon$  and is given by

$$(65) \quad a_{T,l}^\epsilon(\mathbf{u}, \mathbf{v}) = \frac{f''(0)}{\epsilon^{d+1}\omega_d} \int_D \int_D \omega(\mathbf{x})\omega(\mathbf{y})J^\epsilon(|\mathbf{y}-\mathbf{x}|)|\mathbf{y}-\mathbf{x}|S(\mathbf{y},\mathbf{x};\mathbf{u})S(\mathbf{y},\mathbf{x};\mathbf{v})d\mathbf{y}d\mathbf{x}.$$

Similarly, linearization of  $\mathcal{L}_D^\epsilon$  in Equation 14 gives

$$(66) \quad \mathcal{L}_{D,l}^\epsilon(\mathbf{u})(\mathbf{x}) = \frac{g''(0)}{\epsilon^{d+2}\omega_d} \int_{H_\epsilon(\mathbf{x})} \omega(\mathbf{x})\omega(\mathbf{y})J^\epsilon(|\mathbf{y}-\mathbf{x}|) [\theta(\mathbf{y},t;\mathbf{u}) + \theta(\mathbf{x},t;\mathbf{u})] \mathbf{e}_{\mathbf{y}-\mathbf{x}} d\mathbf{y}.$$

The associated bilinear form is given by

$$(67) \quad a_{D,l}^\epsilon(\mathbf{u}, \mathbf{v}) = \frac{g''(0)}{\epsilon^2} \int_D \omega(\mathbf{x})\theta(\mathbf{x};\mathbf{u})\theta(\mathbf{y};\mathbf{v})d\mathbf{x}.$$

The total force after linearization is

$$(68) \quad \mathcal{L}_l^\epsilon(\mathbf{u})(\mathbf{x}) = \mathcal{L}_{T,l}^\epsilon(\mathbf{u})(\mathbf{x}) + \mathcal{L}_{D,l}^\epsilon(\mathbf{u})(\mathbf{x})$$

and the bilinear operator associated to  $\mathcal{L}_l^\epsilon$  is given by

$$(69) \quad a_l^\epsilon(\mathbf{u}, \mathbf{v}) = a_{T,l}^\epsilon(\mathbf{u}, \mathbf{v}) + a_{D,l}^\epsilon(\mathbf{u}, \mathbf{v}).$$

We have

$$(\mathcal{L}_l^\epsilon(\mathbf{u}), \mathbf{v}) = -a_l^\epsilon(\mathbf{u}, \mathbf{v}).$$

We now discuss the stability of the FEM approximation to the linearized problem. Let  $\mathbf{u}_{l,h}^k$  denote the approximate solution satisfying, for  $k \geq 1$ ,

$$(70) \quad \left( \frac{\mathbf{u}_{l,h}^{k+1} - 2\mathbf{u}_{l,h}^k + \mathbf{u}_{l,h}^{k-1}}{\Delta t^2}, \tilde{\mathbf{u}} \right) = (\mathcal{L}_l^\epsilon(\mathbf{u}_{l,h}^k), \tilde{\mathbf{u}}) + (\mathbf{b}_h^k, \tilde{\mathbf{u}}), \quad \forall \tilde{\mathbf{u}} \in V_h$$



and, for  $k = 0$ ,

$$(71) \quad \left( \frac{\mathbf{u}_{l,h}^1 - \mathbf{u}_{l,h}^0}{\Delta t^2}, \tilde{\mathbf{u}} \right) = \frac{1}{2} (\mathcal{L}^\epsilon(\mathbf{u}_{l,h}^0), \tilde{\mathbf{u}}) + \frac{1}{\Delta t} (\mathbf{v}_{l,h}^0, \tilde{\mathbf{u}}) + \frac{1}{2} (\mathbf{b}_h^0, \tilde{\mathbf{u}}), \quad \forall \tilde{\mathbf{u}} \in V_h.$$

The following notation will be used to define the discrete energy at each time step  $k$

$$(72) \quad \begin{aligned} \bar{\mathbf{u}}_h^{k+1} &:= \frac{\mathbf{u}_h^{k+1} + \mathbf{u}_h^k}{2}, \quad \bar{\mathbf{u}}_h^k := \frac{\mathbf{u}_h^k + \mathbf{u}_h^{k-1}}{2}, \\ \bar{\partial}_t^+ \mathbf{u}_h^k &:= \frac{\mathbf{u}_h^{k+1} - \mathbf{u}_h^{k-1}}{2\Delta t}, \quad \bar{\partial}_t^+ \mathbf{u}_h^k := \frac{\mathbf{u}_h^{k+1} - \mathbf{u}_h^k}{\Delta t}, \quad \bar{\partial}_t^- \mathbf{u}_h^k := \frac{\mathbf{u}_h^k - \mathbf{u}_h^{k-1}}{\Delta t}. \end{aligned}$$

We also define

$$\bar{\partial}_{tt} \mathbf{u}_h^k := \frac{\mathbf{u}_h^{k+1} - 2\mathbf{u}_h^k + \mathbf{u}_h^{k-1}}{\Delta t^2} = \frac{\bar{\partial}_t^+ \mathbf{u}_h^k - \bar{\partial}_t^- \mathbf{u}_h^k}{\Delta t}.$$

We introduce the discrete energy associated with  $\mathbf{u}_{l,h}^k$  at time step  $k$  as follows

$$\mathcal{E}(\mathbf{u}_{l,h}^k) := \frac{1}{2} \left[ \|\bar{\partial}_t^+ \mathbf{u}_{l,h}^k\|^2 - \frac{\Delta t^2}{4} a_l^\epsilon(\bar{\partial}_t^+ \mathbf{u}_{l,h}^k, \bar{\partial}_t^+ \mathbf{u}_{l,h}^k) + a_l^\epsilon(\bar{\mathbf{u}}_{l,h}^{k+1}, \bar{\mathbf{u}}_{l,h}^{k+1}) \right]$$

Following [Theorem 4.1, [Karaa, 2012]], the stability of central difference scheme is given by

**THEOREM 9. Energy Stability of the Central difference approximation of linearized peridynamics**  
 Let  $\mathbf{u}_{l,h}^k$  be the approximate solution of Equation 70 and Equation 71. In the absence of body force  $\mathbf{b}(t) = 0$  for all  $t$ , if  $\Delta t$  satisfies the CFL like condition

$$(73) \quad \frac{\Delta t^2}{4} \sup_{\mathbf{u} \in V_h \setminus \{0\}} \frac{a_l^\epsilon(\mathbf{u}, \mathbf{u})}{(\mathbf{u}, \mathbf{u})} \leq 1,$$

then the discrete energy is positive and we have the stability

$$(74) \quad \mathcal{E}(\mathbf{u}_{l,h}^k) = \mathcal{E}(\mathbf{u}_{l,h}^0).$$

We skip the proof of above theorem as it is straight-forward extension of Theorem 5.2 in [Jha and Lipton, 2017].

**5. Numerical experiments.** In this section, we present numerical simulations that are consistent with the theoretical a-priori bound on the convergence rate. We also compare the peridynamic energy of the material softening zone and the classic Griffith's fracture energy of linear elastic fracture mechanics.

We consider Plexiglass at room temperature and specify the density  $\rho = 1200 \text{ kg/m}^3$ , bulk modulus  $K = 25 \text{ GPa}$ , Poisson's ratio  $\nu = 0.245$ , and critical energy release rate  $G_c = 500 \text{ Jm}^{-2}$ . The pairwise interaction and the hydrostatic interaction are characterized by potentials  $f(r) = c(1 - \exp[-\beta r^2])$  and  $g(r) = \bar{C}r^2/2$  respectively. Here we have used a quadratic hydrostatic interaction potential. The influence function is  $J(r) = 1 - r$ . Since pairwise potential  $f$  is symmetric for positive and negative strain the critical strain is given by  $S_c(\mathbf{y}, bx) = \frac{\pm \bar{r}}{\sqrt{\mathbf{y} \cdot \mathbf{x}}}$ , where  $\pm \bar{r}$  is the inflection point of  $f(r)$  given by  $\bar{r} = \frac{1}{\sqrt{\beta}}$ . Following equations 94, 95, and 97 of [Lipton et al., 2018b], the relation between peridynamic material

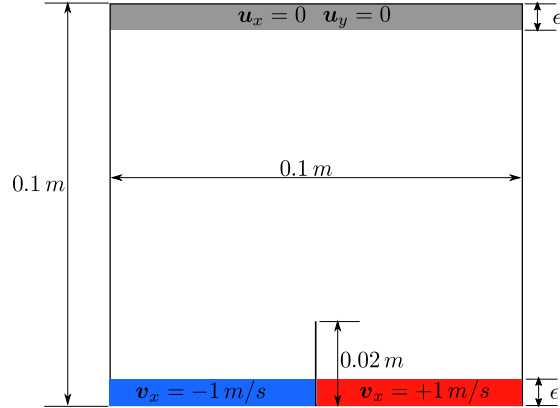


Fig. 3: Material domain  $D = [0, 0.1 m]^2$  with crack of length  $0.02 m$ . The x-component and y-component of displacement are fixed along a collar of thickness equal to the horizon on top. On the bottom the velocity  $\mathbf{v}_x = \pm 1 m/s$  along x-direction is specified on either side of the crack to make the crack propagate upwards.

parameters and Lamé constants  $(\lambda, \mu)$  and critical energy release rate  $G_c$  can be written as (for 2-d)

$$(75) \quad c = \frac{\pi G_c}{4M_J}, \quad \beta = \frac{4\mu}{CM_J}, \quad \bar{C} = \frac{2(\lambda - \mu)}{M_J^2},$$

where  $M_J$  is given by

$$M_J = \int_0^1 J(r)r^2 dr = \frac{1}{12}.$$

By solving Equation 75, we get  $c = 4712.4$ ,  $\bar{C} = -1.7349 \times 10^{11}$ ,  $\beta = 1.5647 \times 10^8$ .

We consider a 2-d domain  $D = [0, 0.1 m]^2$  (with unit thickness in third direction) with vertical crack of length  $0.02 m$ . The boundary conditions are described in Figure 3. The simulation time is  $T = 40 \mu s$  and the time step is  $\Delta t = 0.004 \mu s$ . We consider two horizons  $8 mm$  and  $4 mm$ . We run simulations for mesh sizes  $h = 2, 1, 0.5 mm$ . We consider the central difference time discretization described by Equation 41 on a uniform mesh consisting of linear triangle elements. Second order quadrature approximation is used in the simulation for each triangle element. To reduce the load on memory and to avoid matrix-vector multiplication at each time step, we approximate the mass matrix by diagonal mass matrix using lumping (row-sum) technique. Suppose exact mass matrix is  $\mathbf{M} = [m_{ij}]$  where  $m_{ij}$  is the element of  $\mathbf{M}$  corresponding to  $i^{\text{th}}$  row and  $j^{\text{th}}$  column, then we approximate  $\mathbf{M}$  by diagonal matrix  $\hat{\mathbf{M}} = [\hat{m}_{ij}]$  where  $\hat{m}_{ii} = \sum_j m_{ij}$  and  $\hat{m}_{ij} = 0$  if  $j \neq i$ .

**5.1. Convergence rate.** To compute convergence rate numerically we proceed as follows: consider a fixed horizon  $\epsilon$  and three different mesh sizes  $h_1, h_2, h_3$  such that  $r = h_1/h_2 = h_2/h_3$ . Let  $\mathbf{u}_1, \mathbf{u}_2, \mathbf{u}_3$  be approximate solutions corresponding to meshes of size  $h_1, h_2, h_3$ , and let  $\mathbf{u}$  be the exact solution. We write the error as  $\|\mathbf{u}_h - \mathbf{u}\| = Ch^\alpha$  for some constant  $C$  and  $\alpha > 0$ , to get

$$\begin{aligned} \log(\|\mathbf{u}_1 - \mathbf{u}_2\|) &= C + \alpha \log h_2, \\ \log(\|\mathbf{u}_2 - \mathbf{u}_3\|) &= C + \alpha \log h_3. \end{aligned}$$

From above two equations, it is easy to see that the rate of convergence  $\alpha$  is

$$(76) \quad \frac{\log(\|\mathbf{u}_1 - \mathbf{u}_2\|) - \log(\|\mathbf{u}_2 - \mathbf{u}_3\|)}{\log(r)}.$$

The convergence result for horizons  $\epsilon = 8 \text{ mm}$  and  $\epsilon = 4 \text{ mm}$  is shown in [Figure 4](#). In the simulation we have considered second order approximation of integration using quadrature points. The simulations show a rate of convergence that agrees with the a-priori estimates given in [Theorem 6](#).

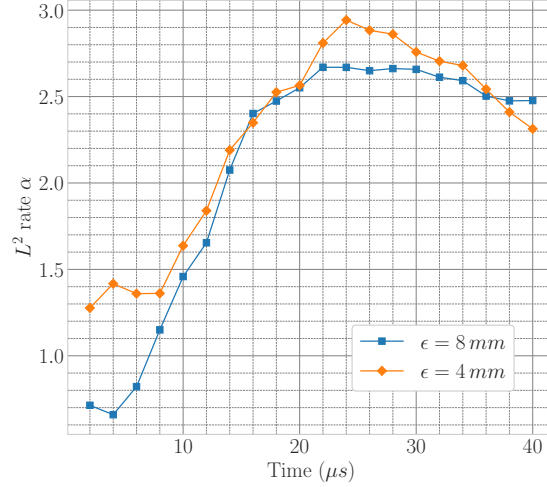


Fig. 4: Convergence rate at different times for two horizons. For both horizons  $\epsilon = 4, 8 \text{ mm}$ , the three meshes of size  $h = 2, 1, 0.5 \text{ mm}$  were considered to compute the convergence rate.

**5.2. Fracture energy of crack zone.** The extent of damage at material point  $\mathbf{x}$  is given by the function  $Z(\mathbf{x})$

$$(77) \quad Z(\mathbf{x}) = \max_{\mathbf{y} \in H_\epsilon(\mathbf{x}) \cap D} \frac{S(\mathbf{y}, \mathbf{x}; \mathbf{u})}{S_c^+}.$$

The crack zone is defined as set of material points which have  $Z > 1$ . We compute the peridynamic energy of crack zone and compare it with the Griffith's fracture energy. For a crack of length  $l$ , the Griffith's fracture energy (G.E.) will be  $G.E. = G_c \times l$ . The peridynamic fracture energy (P.E.) associated with the material softening zone is given by

$$P.E. = \int_{\substack{\mathbf{x} \in D, \\ Z(\mathbf{x}) \geq 1}} \left[ \frac{1}{\epsilon^d \omega_d} \int_{H_\epsilon(\mathbf{x})} |\mathbf{y} - \mathbf{x}| \mathcal{W}^\epsilon(S(\mathbf{y}, \mathbf{x}; \mathbf{u})) d\mathbf{y} \right] d\mathbf{x} \\ + \int_{\substack{\mathbf{x} \in D, \\ Z(\mathbf{x}) \geq 1}} \mathcal{V}^\epsilon(\theta(\mathbf{x}, t; \mathbf{u})) d\mathbf{x}$$

where  $\mathcal{W}^\epsilon(S(\mathbf{y}, \mathbf{x}; \mathbf{u}))$  is the bond-based potential, see [Equation 2](#) and  $\mathcal{V}^\epsilon(\theta(\mathbf{x}, t; \mathbf{u}))$  is the hydrostatic interaction potential, see [Equation 4](#).

In [Figure 5](#) classical fracture energy and peridynamic fracture energy is shown at different crack length. The error in both energies at different times is shown in [Figure 6](#). The agreement between two energies is good. The damage profile at time  $30 \mu s$  and  $40 \mu s$  is shown in [Figure 7](#). At each node, the damage function  $Z$  is computed by treating edges between mesh nodes as bonds. In addition to the damage plots, we show velocity profile at  $30 \mu s$  and  $40 \mu s$  in [Figure 8](#). In [Figure 9](#) we show the plot of the  $xx$  component of symmetric gradient of the displacement. Here the region for which the magnitude of the strain is greater than a multiple of the critical strain is the yellow region. It is seen that the high strain region surrounds the crack.

As the crack is propagating vertically it is seen that the high strain region is next to the crack i

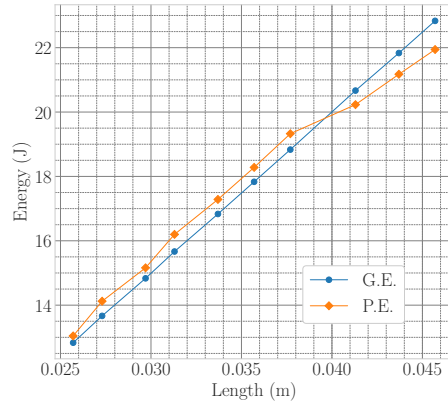


Fig. 5: Peridynamic energy and Griffith's energy as a function of crack length.

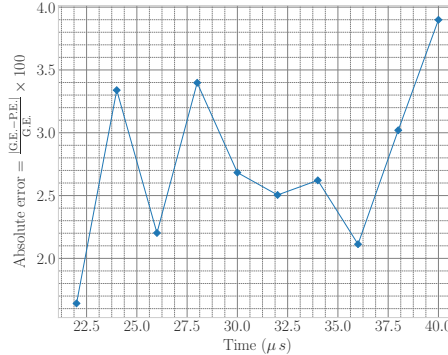


Fig. 6: Error between Peridynamic energy and Griffith's energy at different times.

**6. Lipschitz continuity of peridynamic force and higher temporal regularity of solutions.** In this section, we prove [Theorem 1](#) and [Theorem 3](#). Here  $\mathbf{u} \in W \subset H^2(D; \mathbb{R}^d)$  and the  $\|\mathbf{u}\|_2$  norm is given by

$$(78) \quad \|\mathbf{u}\|_2 = \|\mathbf{u}\| + \|\nabla \mathbf{u}\| + \|\nabla^2 \mathbf{u}\|.$$

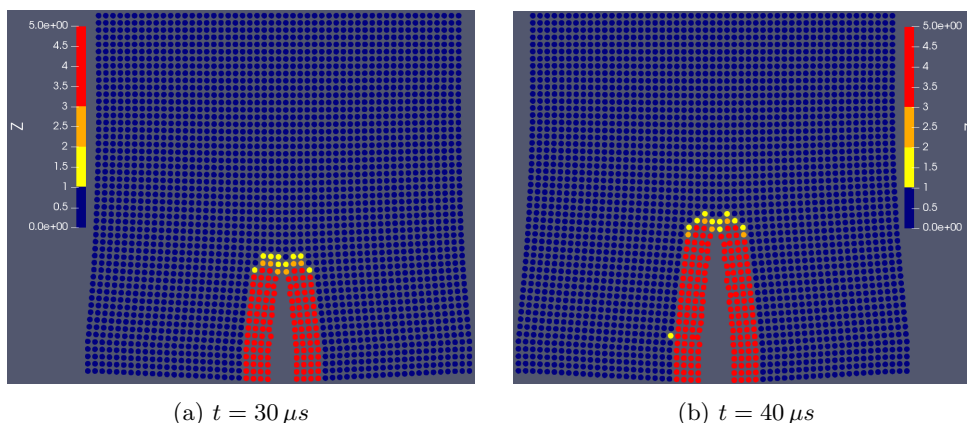


Fig. 7: Color plot of damage function  $Z$  on deformed material domain at time  $t = 30 \mu s$  and  $40 \mu s$ . Dark blue represents undamaged material  $Z < 1$ ,  $Z \approx 1$  is yellow at crack tip, red is softening material. Here, the displacements are scaled by 100 and damage function is cut off at 5 to highlight the crack zone.

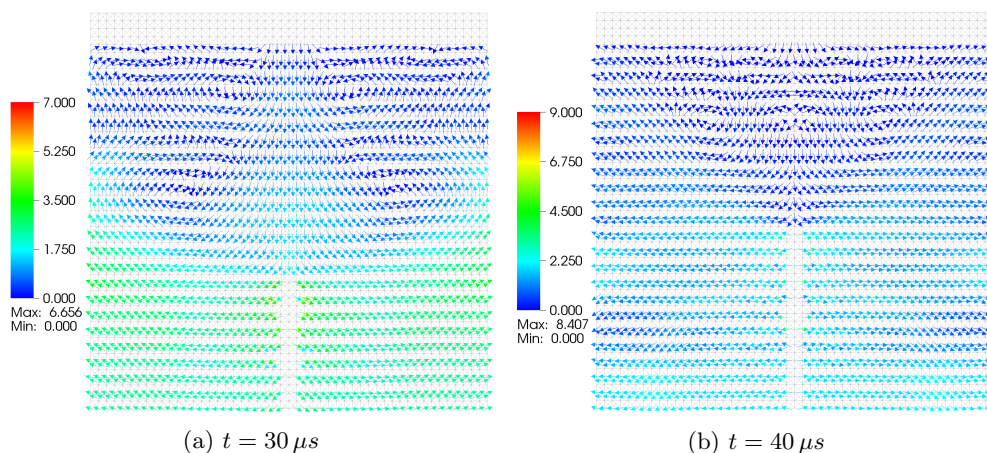


Fig. 8: Velocity profile.

**6.1. Proof of Lipschitz continuity with respect to the  $\|\cdot\|_2$  norm.** We assume that the potential function  $f$  satisfies  $C_i^f < \infty$  for  $i = 0, 1, 2, 3, 4$ . Recall that  $C_0^f = \sup_r |f(r)|$  and  $C_i^f = \sup_r |f^{(i)}(r)|$  for  $i = 1, \dots, 4$ .  $C_i^g$  is defined similarly for  $i = 0, 1, \dots, 4$ . If the potential function  $g$  is a convex-concave function then we can assume  $C_i^g < \infty$  for  $i = 0, 1, 2, 3, 4$ . In what follows, we will prove the [Theorem 1](#) for convex-concave type  $g$ . If  $g$  is a purely a quadratic function the proof follows easily using only a subset of the estimates proved in this section.

Let  $\mathbf{u}, \mathbf{v} \in W$ . Using the triangle inequality, we get

$$(79) \quad \|\mathcal{L}^\epsilon(\mathbf{u}) - \mathcal{L}^\epsilon(\mathbf{v})\|_2 \leq \|\mathcal{L}_T^\epsilon(\mathbf{u}) - \mathcal{L}_T^\epsilon(\mathbf{v})\|_2 + \|\mathcal{L}_D^\epsilon(\mathbf{u}) - \mathcal{L}_D^\epsilon(\mathbf{v})\|_2,$$

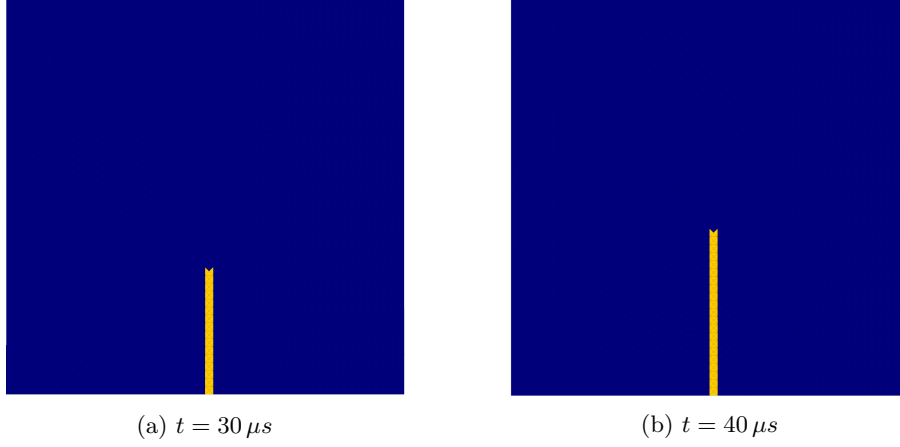


Fig. 9: Magnitude of the  $xx$  component of strain  $\nabla \mathbf{u} + \nabla \mathbf{u}^T$ . The region for which the magnitude of the strain is greater than a multiple of the critical strain is the yellow region

where  $\mathcal{L}_T^\epsilon$  and  $\mathcal{L}_D^\epsilon$  is given by [Equation 13](#) and [Equation 14](#).

We first write the peridynamic force  $\mathcal{L}_T^\epsilon(\mathbf{u})(\mathbf{x})$  as follows

$$(80) \quad \begin{aligned} & \mathcal{L}_T^\epsilon(\mathbf{u})(\mathbf{x}) \\ &= \frac{2}{\epsilon^{d+1}\omega_d} \int_{H_\epsilon(\mathbf{x})} \omega(\mathbf{x})\omega(\mathbf{y}) \frac{J^\epsilon(|\mathbf{y}-\mathbf{x}|)}{\sqrt{|\mathbf{y}-\mathbf{x}|}} f'(\sqrt{|\mathbf{y}-\mathbf{x}|}S(\mathbf{y}, \mathbf{x}; \mathbf{u})) \mathbf{e}_{\mathbf{y}-\mathbf{x}} d\mathbf{y}, \end{aligned}$$

where we substituted  $\partial_S f(\sqrt{|\mathbf{y}-\mathbf{x}|}S(\mathbf{y}, \mathbf{x}; \mathbf{u})) = \sqrt{|\mathbf{y}-\mathbf{x}|} f'(\sqrt{|\mathbf{y}-\mathbf{x}|}S(\mathbf{y}, \mathbf{x}; \mathbf{u}))$ . The form of the peridynamic force described above is the same as the one given in [Section 6, [Jha and Lipton, 2017](#)]. We apply Theorem 3.1 in [[Jha and Lipton, 2017](#)] to show

$$(81) \quad \begin{aligned} \|\mathcal{L}_T^\epsilon(\mathbf{u}) - \mathcal{L}_T^\epsilon(\mathbf{v})\|_2 &\leq \frac{L_1(1 + (\|\mathbf{u}\|_2 + \|\mathbf{v}\|_2) + (\|\mathbf{u}\|_2 + \|\mathbf{v}\|_2)^2)}{\epsilon^3} \|\mathbf{u} - \mathbf{v}\|_2 \\ &\leq \frac{L_1(1 + \|\mathbf{u}\|_2 + \|\mathbf{v}\|_2)^2}{\epsilon^3} \|\mathbf{u} - \mathbf{v}\|_2 \end{aligned}$$

and

$$(82) \quad \|\mathcal{L}_T^\epsilon(\mathbf{u})\|_2 \leq \frac{L_2(\|\mathbf{u}\|_2 + \|\mathbf{u}\|_2^2)}{\epsilon^{5/2}}.$$

Next we analyze  $\|\mathcal{L}_D^\epsilon(\mathbf{u}) - \mathcal{L}_D^\epsilon(\mathbf{v})\|_2$ . We define new terms to simplify the calculations. For  $\boldsymbol{\xi} \in H_1(\mathbf{0})$ , we set

$$(83) \quad \begin{aligned} s_\xi &= \epsilon|\boldsymbol{\xi}|, \quad \mathbf{e}_\xi = \frac{\boldsymbol{\xi}}{|\boldsymbol{\xi}|}, \\ \omega_\xi(\mathbf{x}) &= \omega(\mathbf{x} + \epsilon\boldsymbol{\xi})\omega(\mathbf{x}), \\ \bar{\mathbf{u}}_\xi(\mathbf{x}) &= \mathbf{u}(\mathbf{x} + \epsilon\boldsymbol{\xi}) - \mathbf{u}(\mathbf{x}), \\ (\mathbf{u} - \mathbf{v})(\mathbf{x}) &= \mathbf{u}(\mathbf{x}) - \mathbf{v}(\mathbf{x}). \end{aligned}$$

Similar notations hold if we exchange  $\mathbf{x}$ ,  $\boldsymbol{\xi} \in H_1(\mathbf{0})$ , and  $\mathbf{u} \in W$  by  $\mathbf{y}$ ,  $\boldsymbol{\eta} \in H_1(\mathbf{0})$ , and  $\mathbf{v} \in W$  respectively. We will also encounter various moments of the influence function  $J$  therefore we define following moments

$$(84) \quad \bar{J}_\alpha = \frac{1}{\omega_d} \int_{H_1(\mathbf{0})} J(|\boldsymbol{\xi}|) |\boldsymbol{\xi}|^{-\alpha} d\boldsymbol{\xi}, \quad \text{for } \alpha \in \mathbb{R}.$$

Recall that  $J(|\boldsymbol{\xi}|) = 0$  for  $\boldsymbol{\xi} \notin H_1(\mathbf{0})$  and  $0 \leq J(|\boldsymbol{\xi}|) \leq M$  for  $\boldsymbol{\xi} \in H_1(\mathbf{0})$ . The boundary function  $\omega$  is assumed to satisfy

$$(85) \quad \sup_{\mathbf{x}} |\nabla \omega(\mathbf{x})| < \infty, \quad \sup_{\mathbf{x}} |\nabla^2 \omega(\mathbf{x})| < \infty.$$

We choose finite constants  $C_{\omega_1}$  and  $C_{\omega_2}$  such that

$$(86) \quad \begin{aligned} |\nabla \omega_{\boldsymbol{\xi}}(\mathbf{x})| &\leq C_{\omega_1}, & |\nabla \omega(\mathbf{x})| &\leq C_{\omega_1}, \\ |\nabla^2 \omega_{\boldsymbol{\xi}}(\mathbf{x})| &\leq C_{\omega_2}, & |\nabla^2 \omega(\mathbf{x})| &\leq C_{\omega_2}. \end{aligned}$$

We now collect the following estimates which will be used to estimate  $\|\mathcal{L}_D^\epsilon(\mathbf{u}) - \mathcal{L}_D^\epsilon(\mathbf{v})\|_2$ .

LEMMA 10. *Let  $\mathbf{u}, \mathbf{v} \in W$ , for any  $\boldsymbol{\eta} \in H_1(\mathbf{0})$  and  $\delta \leq 2\epsilon$ , we have*

$$(87) \quad \sup_{\mathbf{x} \in D} |\theta(\mathbf{x}; \mathbf{u})| \leq 2C_{e_1} \bar{J}_0 \|\mathbf{u}\|_2,$$

$$(88) \quad \int_D |\theta(\mathbf{x} + \delta\boldsymbol{\eta}; \mathbf{u})|^2 d\mathbf{x} \leq 4\bar{J}_0^2 \|\mathbf{u}\|_2^2,$$

$$(89) \quad \int_D |\nabla \theta(\mathbf{x} + \delta\boldsymbol{\eta}; \mathbf{u})|^2 d\mathbf{x} \leq 8\bar{J}_0^2 (1 + C_{\omega_1})^2 \|\mathbf{u}\|_2^2,$$

$$(90) \quad \int_D |\theta(\mathbf{x} + \delta\boldsymbol{\eta}; \mathbf{u} - \mathbf{v})|^2 |\nabla \theta(\mathbf{x} + \delta\boldsymbol{\eta}; \mathbf{v})|^2 d\mathbf{x} \leq 32\bar{J}_0^4 (1 + C_{\omega_1})^2 \|\mathbf{v}\|_2^2 \|\mathbf{u} - \mathbf{v}\|_2^2,$$

$$(91) \quad \int_D |\nabla \theta(\mathbf{x} + \delta\boldsymbol{\eta}; \mathbf{u})|^4 d\mathbf{x} \leq 128\bar{J}_0^4 (C_{e_2}^2 + C_{e_1} C_{\omega_1}^2) \|\mathbf{u}\|_2^4,$$

$$(92) \quad \int_D |\theta(\mathbf{x} + \delta\boldsymbol{\eta}; \mathbf{u} - \mathbf{v})|^2 |\nabla \theta(\mathbf{x} + \delta\boldsymbol{\eta}; \mathbf{v})|^4 d\mathbf{x} \leq 512\bar{J}_0^6 C_{e_1}^2 (C_{e_2}^2 + C_{e_1} C_{\omega_1}^2) \|\mathbf{u} - \mathbf{v}\|_2^2 \|\mathbf{v}\|_2^4,$$

$$(93) \quad \int_D |\nabla^2 \theta(\mathbf{x} + \delta\boldsymbol{\eta}; \mathbf{u})|^2 d\mathbf{x} \leq 16\bar{J}_0^2 (1 + 2C_{\omega_1} + C_{\omega_2})^2 \|\mathbf{u}\|_2^2.$$

Here  $\nabla$  in all the equations above is with respect to  $\mathbf{x}$ . The constants  $C_{e_1}, C_{e_2}$  are the constants associated to the Sobolev embedding property of space  $H^2(D; \mathbb{R}^d)$ , see [Equation 18](#) and [Equation 19](#).

*Proof.* Using the notation given in [Equation 83](#), we write  $\theta(\mathbf{x}; \mathbf{u})$  as

$$(94) \quad \theta(\mathbf{x}; \mathbf{u}) = \frac{1}{\omega_d} \int_{H_1(\mathbf{0})} \omega(\mathbf{x} + \epsilon\boldsymbol{\xi}) J(|\boldsymbol{\xi}|) \bar{\mathbf{u}}_{\boldsymbol{\xi}}(\mathbf{x}) \cdot \mathbf{e}_{\boldsymbol{\xi}} d\boldsymbol{\xi}.$$

On noting that  $|\bar{\mathbf{u}}_{\boldsymbol{\xi}}(\mathbf{x})| \leq 2\|\mathbf{u}\|_\infty$  and  $\|\mathbf{u}\|_\infty \leq C_{e_1} \|\mathbf{u}\|_2$ , we easily see that

$$(95) \quad |\theta(\mathbf{x}; \mathbf{u})| \leq \bar{J}_0 2 \|\mathbf{u}\|_\infty \leq 2C_{e_1} \bar{J}_0 \|\mathbf{u}\|_2.$$

In the rest of the proof, we will let  $\mathbf{y} = \mathbf{x} + \delta\boldsymbol{\eta}$ , where  $0 \leq \delta \leq 2\epsilon$  and  $\boldsymbol{\eta} \in H_1(\mathbf{0})$ .

To show [Equation 88](#), we first introduce an important identity which will be used frequently. Let  $p(\boldsymbol{\xi})$  be some function of  $\boldsymbol{\xi}$ , and  $\alpha, C \in \mathbb{R}$  then

$$\begin{aligned}
& \left| \frac{C}{\omega_d} \int_{H_1(\mathbf{0})} \frac{J(|\boldsymbol{\xi}|)}{|\boldsymbol{\xi}|^\alpha} p(\boldsymbol{\xi}) d\boldsymbol{\xi} \right|^2 \\
&= \left( \frac{C}{\omega_d} \right)^2 \int_{H_1(\mathbf{0})} \int_{H_1(\mathbf{0})} \frac{J(|\boldsymbol{\xi}|)}{|\boldsymbol{\xi}|^\alpha} \frac{J(|\boldsymbol{\eta}|)}{|\boldsymbol{\eta}|^\alpha} p(\boldsymbol{\xi}) p(\boldsymbol{\eta}) d\boldsymbol{\xi} d\boldsymbol{\eta} \\
&\leq \left( \frac{C}{\omega_d} \right)^2 \int_{H_1(\mathbf{0})} \int_{H_1(\mathbf{0})} \frac{J(|\boldsymbol{\xi}|)}{|\boldsymbol{\xi}|^\alpha} \frac{J(|\boldsymbol{\eta}|)}{|\boldsymbol{\eta}|^\alpha} \frac{p(\boldsymbol{\xi})^2 + p(\boldsymbol{\eta})^2}{2} d\boldsymbol{\xi} d\boldsymbol{\eta} \\
(96) \quad &= C^2 \frac{\bar{J}_\alpha}{\omega_d} \int_{H_1(\mathbf{0})} \frac{J(|\boldsymbol{\xi}|)}{|\boldsymbol{\xi}|^\alpha} p(\boldsymbol{\xi})^2 d\boldsymbol{\xi},
\end{aligned}$$

where we used the inequality  $ab \leq a^2/2 + b^2/2$  in the first step, and definition of  $\bar{J}_\alpha$  and symmetry of terms in second step.

From the expression of  $\theta(\mathbf{y}; \mathbf{u})$  we can show

$$(97) \quad \int_D |\theta(\mathbf{y}; \mathbf{u})|^2 d\mathbf{x} \leq 4\bar{J}_0^2 \|\mathbf{u}\|^2 \leq 4\bar{J}_0^2 \|\mathbf{u}\|_2^2.$$

We now prove the bound [Equation 89](#). Taking the gradient of  $\theta(\mathbf{y}; \mathbf{u})$ , with respect to  $\mathbf{x}$ , noting that  $\mathbf{y} = \mathbf{x} + \delta\boldsymbol{\eta}$ , we get

$$\begin{aligned}
(98) \quad \nabla\theta(\mathbf{y}; \mathbf{u}) &= \frac{1}{\omega_d} \int_{H_1(\mathbf{0})} J(|\boldsymbol{\xi}|) \omega(\mathbf{y} + \epsilon\boldsymbol{\xi}) (\nabla\bar{\mathbf{u}}_\xi(\mathbf{y}))^T \mathbf{e}_\xi d\boldsymbol{\xi} \\
&\quad + \frac{1}{\omega_d} \int_{H_1(\mathbf{0})} J(|\boldsymbol{\xi}|) \nabla\omega(\mathbf{y} + \epsilon\boldsymbol{\xi}) \bar{\mathbf{u}}_\xi(\mathbf{y}) \cdot \mathbf{e}_\xi d\boldsymbol{\xi}.
\end{aligned}$$

We can show using inequality [Equation 96](#) and the estimates  $\int_D |\nabla\bar{\mathbf{u}}_\xi(\mathbf{y})|^2 d\mathbf{x} \leq 4\|\nabla\mathbf{u}\|^2 \leq 4\|\mathbf{u}\|_2^2$ ,  $|\nabla\omega(\mathbf{y} + \epsilon\boldsymbol{\xi})| \leq C_{\omega_1}$ ,  $\int_D |\bar{\mathbf{u}}_\xi(\mathbf{y})|^2 d\mathbf{x} \leq 4\|\mathbf{u}\|_2^2$ , to conclude

$$\begin{aligned}
(99) \quad \int_D |\nabla\theta(\mathbf{y}; \mathbf{u})|^2 d\mathbf{x} &\leq \frac{2\bar{J}_0}{\omega_d} \int_{H_1(\mathbf{0})} J(|\boldsymbol{\xi}|) 4\|\mathbf{u}\|_2^2 d\boldsymbol{\xi} + \frac{2\bar{J}_0}{\omega_d} \int_{H_1(\mathbf{0})} J(|\boldsymbol{\xi}|) 4C_{\omega_1}^2 \|\mathbf{u}\|_2^2 d\boldsymbol{\xi} \\
&= 8\bar{J}_0^2 (1 + C_{\omega_1}^2) \|\mathbf{u}\|_2^2 \leq 8\bar{J}_0^2 (1 + C_{\omega_1})^2 \|\mathbf{u}\|_2^2.
\end{aligned}$$

We now show [Equation 90](#). We will use [Equation 87](#) and [Equation 89](#), and proceed as follows

$$\begin{aligned}
(100) \quad & \int_D |\theta(\mathbf{y}; \mathbf{u} - \mathbf{v})|^2 |\nabla\theta(\mathbf{y}; \mathbf{v})|^2 d\mathbf{x} \\
&\leq \left( \sup_{\mathbf{y}} |\theta(\mathbf{y}; \mathbf{u} - \mathbf{v})| \right)^2 \int_D |\nabla\theta(\mathbf{y}; \mathbf{v})|^2 d\mathbf{x} \\
&\leq 32\bar{J}_0^4 (1 + C_{\omega_1})^2 \|\mathbf{v}\|_2^2 \|\mathbf{u} - \mathbf{v}\|_2^2.
\end{aligned}$$

To prove [Equation 91](#) we note expression of  $\nabla\theta(\mathbf{y}; \mathbf{u})$  in [Equation 98](#) and inequality  $(a + b)^4 \leq 8a^4 + 8b^4$  and [Equation 96](#) to get

$$\begin{aligned}
(101) \quad |\nabla\theta(\mathbf{y}; \mathbf{u})|^4 &\leq \frac{64\bar{J}_0^3}{\omega_d} \int_{H_1(\mathbf{0})} J(|\boldsymbol{\xi}|) (|\nabla\mathbf{u}(\mathbf{y} + \epsilon\boldsymbol{\xi})|^4 + |\nabla\mathbf{u}(\mathbf{y})|^4) d\boldsymbol{\xi} \\
&\quad + \frac{64C_{\omega_1}^4 \bar{J}_0^3}{\omega_d} \int_{H_1(\mathbf{0})} J(|\boldsymbol{\xi}|) (|\mathbf{u}(\mathbf{y} + \epsilon\boldsymbol{\xi})|^4 + |\mathbf{u}(\mathbf{y})|^4) d\boldsymbol{\xi}.
\end{aligned}$$



Application of Fubini's theorem gives

$$\begin{aligned}
& \int_D |\nabla\theta(\mathbf{y}; \mathbf{u})|^4 dx \\
& \leq \frac{64\bar{J}_0^3}{\omega_d} \int_{H_1(\mathbf{0})} J(|\xi|) \left( \int_D (|\nabla\mathbf{u}(\mathbf{y} + \epsilon\xi)|^4 + |\nabla\mathbf{u}(\mathbf{y})|^4) dx \right) d\xi \\
& \quad + \frac{64C_{\omega_1}^4 \bar{J}_0^3}{\omega_d} \int_{H_1(\mathbf{0})} J(|\xi|) \left( \int_D (|\mathbf{u}(\mathbf{y} + \epsilon\xi)|^4 + |\mathbf{u}(\mathbf{y})|^4) dx \right) d\xi \\
& \leq \frac{64\bar{J}_0^3}{\omega_d} \int_{H_1(\mathbf{0})} J(|\xi|) \left( 2\|\nabla\mathbf{u}\|_{L^4(D; \mathbb{R}^{d \times d})}^4 \right) d\xi \\
& \quad + \frac{64C_{\omega_1}^4 \bar{J}_0^3}{\omega_d} \int_{H_1(\mathbf{0})} J(|\xi|) \left( \|\mathbf{u}\|_\infty^2 \int_D (|\mathbf{u}(\mathbf{y} + \epsilon\xi)|^2 + |\mathbf{u}(\mathbf{y})|^2) dx \right) d\xi \\
& \leq 128\bar{J}_0^4 \|\nabla\mathbf{u}\|_{L^4(D; \mathbb{R}^{d \times d})}^4 + \frac{64C_{\omega_1}^4 \bar{J}_0^3}{\omega_d} \int_{H_1(\mathbf{0})} J(|\xi|) (\|\mathbf{u}\|_\infty^2 2\|\mathbf{u}\|^2) d\xi \\
(102) \quad & \leq 128\bar{J}_0^4 \|\nabla\mathbf{u}\|_{L^4(D; \mathbb{R}^{d \times d})}^4 + 128C_{\omega_1}^4 \bar{J}_0^4 \|\mathbf{u}\|_\infty^2 \|\mathbf{u}\|^2.
\end{aligned}$$

Using the Sobolev embedding property,  $\|\mathbf{u}\|_\infty \leq C_{e_1} \|\mathbf{u}\|_2$  and  $\|\nabla\mathbf{u}\|_{L^4} \leq C_{e_2} \|\mathbf{u}\|_2$ , we obtain

$$(103) \quad \int_D |\nabla\theta(\mathbf{y}; \mathbf{u})|^4 dx \leq 128\bar{J}_0^4 (C_{e_2}^4 + C_{e_1}^4 C_{\omega_1}^4) \|\mathbf{u}\|_2^4 \leq 128\bar{J}_0^4 (C_{e_2}^2 + C_{e_1} C_{\omega_1}^2)^2 \|\mathbf{u}\|_2^4.$$

The estimate Equation 92 follows by combining estimates Equation 87 and Equation 91. It now remains to show Equation 93. From expression of  $\nabla\theta(\mathbf{y}; \mathbf{u})$  in Equation 98, we have

$$\begin{aligned}
\nabla^2\theta(\mathbf{y}; \mathbf{u}) &= \frac{1}{\omega_d} \int_{H_1(\mathbf{0})} J(|\xi|) \omega(\mathbf{y} + \epsilon\xi) \nabla^2(\bar{\mathbf{u}}_\xi(\mathbf{y}) \cdot \mathbf{e}_\xi) d\xi \\
& \quad + \frac{1}{\omega_d} \int_{H_1(\mathbf{0})} J(|\xi|) ((\nabla(\bar{\mathbf{u}}_\xi(\mathbf{y}))^T \mathbf{e}_\xi) \otimes \nabla\omega(\mathbf{y} + \epsilon\xi)) d\xi \\
& \quad + \frac{1}{\omega_d} \int_{H_1(\mathbf{0})} J(|\xi|) \nabla\omega(\mathbf{y} + \epsilon\xi) \otimes ((\nabla(\bar{\mathbf{u}}_\xi(\mathbf{y}))^T \mathbf{e}_\xi)) d\xi \\
(104) \quad & \quad + \frac{1}{\omega_d} \int_{H_1(\mathbf{0})} J(|\xi|) \nabla^2\omega(\mathbf{y} + \epsilon\xi) \bar{\mathbf{u}}_\xi(\mathbf{y}) \cdot \mathbf{e}_\xi d\xi.
\end{aligned}$$

Using the equation above we can show

$$\begin{aligned}
\int_D |\nabla^2\theta(\mathbf{y}; \mathbf{u})|^2 dx & \leq \frac{3\bar{J}_0}{\omega_d} \int_{H_1(\mathbf{0})} J(|\xi|) \left( \int_D |\nabla^2\bar{\mathbf{u}}_\xi(\mathbf{y})|^2 dx \right) d\xi \\
& \quad + \frac{12C_{\omega_1}^2 \bar{J}_0}{\omega_d} \int_{H_1(\mathbf{0})} J(|\xi|) \left( \int_D |\nabla\bar{\mathbf{u}}_\xi(\mathbf{y})|^2 dx \right) d\xi \\
(105) \quad & \quad + \frac{3C_{\omega_2}^2 \bar{J}_0}{\omega_d} \int_{H_1(\mathbf{0})} J(|\xi|) \left( \int_D |\bar{\mathbf{u}}_\xi(\mathbf{y})|^2 dx \right) d\xi.
\end{aligned}$$

The terms  $|\bar{\mathbf{u}}_\xi(\mathbf{y})|^2$ ,  $|\nabla\bar{\mathbf{u}}_\xi(\mathbf{y})|^2$ , and  $|\nabla^2\bar{\mathbf{u}}_\xi(\mathbf{y})|^2$  are bounded by  $2(|\mathbf{u}(\mathbf{y} + \epsilon\xi)|^2 + |\mathbf{u}(\mathbf{y})|^2)$ ,  $2(|\nabla\mathbf{u}(\mathbf{y} + \epsilon\xi)|^2 + |\nabla\mathbf{u}(\mathbf{y})|^2)$ , and  $2(|\nabla^2\mathbf{u}(\mathbf{y} + \epsilon\xi)|^2 + |\nabla^2\mathbf{u}(\mathbf{y})|^2)$  respectively. Therefore, we have

$$\begin{aligned}
\int_D |\nabla^2\theta(\mathbf{y}; \mathbf{u})|^2 dx & \leq [3\bar{J}_0^2 + 12C_{\omega_1}^2 \bar{J}_0^2 + 3C_{\omega_2}^2 \bar{J}_0^2] 4\|\mathbf{u}\|_2^2 \\
(106) \quad & \leq 16\bar{J}_0^2 (1 + C_{\omega_2} + 2C_{\omega_1})^2 \|\mathbf{u}\|_2^2,
\end{aligned}$$

and this completes the proof of lemma.  $\square$

**Estimating  $\|\mathcal{L}_D^\epsilon(\mathbf{u}) - \mathcal{L}_D^\epsilon(\mathbf{v})\|$ :** We apply the notation described in Equation 83, and write  $\mathcal{L}_D^\epsilon(\mathbf{u})(\mathbf{x})$  as follows

$$(107) \quad \mathcal{L}_D^\epsilon(\mathbf{u})(\mathbf{x}) = \frac{1}{\epsilon^2 \omega_D} \int_{H_1(\mathbf{0})} \omega_\xi(\mathbf{x}) J(|\xi|) [g'(\theta(\mathbf{x} + \epsilon\xi; \mathbf{u})) + g'(\theta(\mathbf{x}; \mathbf{u}))] \mathbf{e}_\xi d\xi.$$

Using the formula above and from the expression for  $\theta$  we can easily show

$$(108) \quad \|\mathcal{L}_D^\epsilon(\mathbf{u}) - \mathcal{L}_D^\epsilon(\mathbf{v})\| \leq \frac{L_1}{\epsilon^2} \|\mathbf{u} - \mathbf{v}\|_2,$$

where  $L_1 = 4C_2^g \bar{J}_0^2$ .

**Estimating  $\|\nabla \mathcal{L}_D^\epsilon(\mathbf{u}) - \nabla \mathcal{L}_D^\epsilon(\mathbf{v})\|$ :** Taking the gradient of Equation 107 gives

$$(109) \quad \begin{aligned} \nabla \mathcal{L}_D^\epsilon(\mathbf{u})(\mathbf{x}) &= \frac{1}{\epsilon^2 \omega_d} \int_{H_1(\mathbf{0})} J(|\xi|) \omega_\xi(\mathbf{x}) \mathbf{e}_\xi \otimes [\nabla g'(\theta(\mathbf{x} + \epsilon\xi; \mathbf{u})) + \nabla g'(\theta(\mathbf{x}; \mathbf{u}))] d\xi \\ &\quad + \frac{1}{\epsilon^2 \omega_d} \int_{H_1(\mathbf{0})} J(|\xi|) \mathbf{e}_\xi \otimes \nabla \omega_\xi(\mathbf{x}) [g'(\theta(\mathbf{x} + \epsilon\xi; \mathbf{u})) + g'(\theta(\mathbf{x}; \mathbf{u}))] d\xi \\ &=: G_1(\mathbf{u})(\mathbf{x}) + G_2(\mathbf{u})(\mathbf{x}), \end{aligned}$$

where we have denoted the first and second term as  $G_1(\mathbf{u})(\mathbf{x})$  and  $G_2(\mathbf{u})(\mathbf{x})$  for convenience. On using the triangle inequality we get

$$\|\nabla \mathcal{L}_D^\epsilon(\mathbf{u}) - \nabla \mathcal{L}_D^\epsilon(\mathbf{v})\| \leq \|G_1(\mathbf{u}) - G_1(\mathbf{v})\| + \|G_2(\mathbf{u}) - G_2(\mathbf{v})\|.$$

From the expression of  $G_1(\mathbf{u})$ , we have

$$\begin{aligned} |G_1(\mathbf{u})(\mathbf{x}) - G_1(\mathbf{v})(\mathbf{x})| &\leq \frac{1}{\epsilon^2 \omega_d} \int_{H_1(\mathbf{0})} J(|\xi|) (|\nabla g'(\theta(\mathbf{x} + \epsilon\xi; \mathbf{u})) - \nabla g'(\theta(\mathbf{x} + \epsilon\xi; \mathbf{v}))| \\ &\quad + |\nabla g'(\theta(\mathbf{x}; \mathbf{u})) - \nabla g'(\theta(\mathbf{x}; \mathbf{v}))|) d\xi. \end{aligned}$$

Let

$$(110) \quad p_1(\mathbf{y}) := |\nabla g'(\theta(\mathbf{y}; \mathbf{u})) - \nabla g'(\theta(\mathbf{y}; \mathbf{v}))|$$

and we get

$$(111) \quad \|G_1(\mathbf{u}) - G_1(\mathbf{v})\|^2 \leq \left(\frac{1}{\epsilon^2}\right)^2 \frac{2\bar{J}_0}{\omega_d} \int_{H_1(\mathbf{0})} J(|\xi|) \left( \int_D (p_1(\mathbf{x} + \epsilon\xi)^2 + p_1(\mathbf{x})^2) d\mathbf{x} \right) d\xi.$$

Note that

$$\nabla g'(\theta(\mathbf{x} + \epsilon\xi; \mathbf{u})) = g''(\theta(\mathbf{x} + \epsilon\xi; \mathbf{u})) \nabla \theta(\mathbf{x} + \epsilon\xi; \mathbf{u}).$$

Therefore, from Equation 110,

$$\begin{aligned} p_1(\mathbf{y}) &= |g''(\theta(\mathbf{y}; \mathbf{u})) \nabla \theta(\mathbf{y}; \mathbf{u}) - g''(\theta(\mathbf{y}; \mathbf{v})) \nabla \theta(\mathbf{y}; \mathbf{v})| \\ &\leq C_2^g |\nabla \theta(\mathbf{y}; \mathbf{u}) - \nabla \theta(\mathbf{y}; \mathbf{v})| + C_3^g |\theta(\mathbf{y}; \mathbf{u}) - \theta(\mathbf{y}; \mathbf{v})| |\nabla \theta(\mathbf{y}; \mathbf{v})| \\ &= C_2^g |\nabla \theta(\mathbf{y}; \mathbf{u} - \mathbf{v})| + C_3^g |\theta(\mathbf{y}; \mathbf{u} - \mathbf{v})| |\nabla \theta(\mathbf{y}; \mathbf{v})|, \end{aligned}$$

where we have added and subtracted  $g''(\theta(\mathbf{y}; \mathbf{u}))\nabla\theta(\mathbf{y}; \mathbf{v})$  and used the fact that  $g''(r) \leq C_2^g$  and  $|g''(r_1) - g''(r_2)| \leq C_3^g|r_1 - r_2|$ . We use the estimate on  $p_1$  and proceed as follows

$$\begin{aligned} \int_D p_1(\mathbf{y})^2 d\mathbf{x} &\leq 2(C_2^g)^2 \int_D |\nabla\theta(\mathbf{y}; \mathbf{u} - \mathbf{v})|^2 d\mathbf{x} \\ &\quad + 2(C_3^g)^2 \int_D |\theta(\mathbf{y}; \mathbf{u} - \mathbf{v})|^2 |\nabla\theta(\mathbf{y}; \mathbf{v})|^2 d\mathbf{x}, \end{aligned}$$

where we denote  $\mathbf{x} + \epsilon\xi$  as  $\mathbf{y}$ . We apply inequality [Equation 89](#) and [Equation 90](#) of [Lemma 10](#) to obtain

$$\begin{aligned} \int_D p_1(\mathbf{y})^2 d\mathbf{x} &\leq 2(C_2^g)^2 8\bar{J}_0^2 (1 + C_{\omega_1})^2 \|\mathbf{u} - \mathbf{v}\|_2^2 \\ &\quad + 2(C_3^g)^2 32\bar{J}_0^4 (1 + C_{\omega_1})^2 \|\mathbf{v}\|_2^2 \|\mathbf{u} - \mathbf{v}\|_2^2 \\ &\leq L_2 (1 + \|\mathbf{v}\|_2)^2 \|\mathbf{u} - \mathbf{v}\|_2^2, \end{aligned}$$

where we have grouped all the constant factors together and denote their product by  $L_2$ . Substituting these estimates in to [Equation 111](#) gives

$$\begin{aligned} \|G_1(\mathbf{u}) - G_1(\mathbf{v})\|^2 &\leq \frac{4L_2\bar{J}_0^2}{\epsilon^4} (1 + \|\mathbf{v}\|_2)^2 \|\mathbf{u} - \mathbf{v}\|_2^2 \\ (112) \quad \Rightarrow \|G_1(\mathbf{u}) - G_1(\mathbf{v})\| &\leq \frac{L_3(1 + \|\mathbf{v}\|_2)}{\epsilon^2} \|\mathbf{u} - \mathbf{v}\|_2, \end{aligned}$$

where we have introduced the new constant  $L_3$ .

The formula for  $G_2(\mathbf{u})$  is similar to  $\mathcal{L}_D^\epsilon(\mathbf{u})$  and therefore we have

$$\|G_2(\mathbf{u}) - G_2(\mathbf{v})\| \leq \frac{C_{\omega_1}L_1}{\epsilon^2} \|\mathbf{u} - \mathbf{v}\|_2.$$

Collecting results, we have shown

$$(113) \quad \|\nabla\mathcal{L}_D^\epsilon(\mathbf{u}) - \nabla\mathcal{L}_D^\epsilon(\mathbf{v})\| \leq \frac{L_4(1 + \|\mathbf{v}\|_2)}{\epsilon^2} \|\mathbf{u} - \mathbf{v}\|_2,$$

where we have introduced new constant  $L_4$ .

**Estimating  $\|\nabla^2\mathcal{L}_D^\epsilon(\mathbf{u}) - \nabla^2\mathcal{L}_D^\epsilon(\mathbf{v})\|$ :** Taking the gradient of [Equation 109](#), gives

$$\begin{aligned} \nabla^2\mathcal{L}_D^\epsilon(\mathbf{u})(\mathbf{x}) &= \frac{1}{\epsilon^2\omega_d} \int_{H_1(\mathbf{0})} \omega_\xi(\mathbf{x}) J(|\xi|) \mathbf{e}_\xi \otimes [\nabla^2 g'(\theta(\mathbf{x} + \epsilon\xi; \mathbf{u})) + \nabla^2 g'(\theta(\mathbf{x}; \mathbf{u}))] d\xi \\ &\quad + \frac{1}{\epsilon^2\omega_d} \int_{H_1(\mathbf{0})} J(|\xi|) \mathbf{e}_\xi \otimes [\nabla g'(\theta(\mathbf{x} + \epsilon\xi; \mathbf{u})) + \nabla g'(\theta(\mathbf{x}; \mathbf{u}))] \otimes \nabla\omega_\xi(\mathbf{x}) d\xi \\ &\quad + \frac{1}{\epsilon^2\omega_d} \int_{H_1(\mathbf{0})} J(|\xi|) \mathbf{e}_\xi \otimes \nabla\omega_\xi(\mathbf{x}) \otimes [\nabla g'(\theta(\mathbf{x} + \epsilon\xi; \mathbf{u})) + \nabla g'(\theta(\mathbf{x}; \mathbf{u}))] d\xi \\ &\quad + \frac{1}{\epsilon^2\omega_d} \int_{H_1(\mathbf{0})} J(|\xi|) \mathbf{e}_\xi \otimes \nabla^2\omega_\xi(\mathbf{x}) [g'(\theta(\mathbf{x} + \epsilon\xi; \mathbf{u})) + g'(\theta(\mathbf{x}; \mathbf{u}))] d\xi \\ (114) \quad &=: H_1(\mathbf{u})(\mathbf{x}) + H_2(\mathbf{u})(\mathbf{x}) + H_3(\mathbf{u})(\mathbf{x}) + H_4(\mathbf{u})(\mathbf{x}). \end{aligned}$$

It is easy to see that estimate on  $\|H_2(\mathbf{u}) - H_2(\mathbf{v})\|$  and  $\|H_3(\mathbf{u}) - H_3(\mathbf{v})\|$  is similar to the estimate for  $\|G_1(\mathbf{u}) - G_1(\mathbf{v})\|$ . Thus, from [Equation 112](#), we have

$$(115) \quad \|H_2(\mathbf{u}) - H_2(\mathbf{v})\| + \|H_3(\mathbf{u}) - H_3(\mathbf{v})\| \leq \frac{2C_{\omega_1}L_3(1 + \|\mathbf{v}\|_2)}{\epsilon^2} \|\mathbf{u} - \mathbf{v}\|_2.$$

Also the estimate for  $\|H_4(\mathbf{u}) - H_4(\mathbf{v})\|$  is similar to the estimate for  $\|G_2(\mathbf{u}) - G_2(\mathbf{v})\|$  and we conclude

$$(116) \quad \|H_4(\mathbf{u}) - H_4(\mathbf{v})\| \leq \frac{C_{\omega_2} L_1}{\epsilon^2} \|\mathbf{u} - \mathbf{v}\|_2.$$

We now work on  $\|H_1(\mathbf{u}) - H_1(\mathbf{v})\|$ . From expression of  $H_1(\mathbf{u})(\mathbf{x})$  in Equation 114, we can easily get following

$$(117) \quad \begin{aligned} |H_1(\mathbf{u})(\mathbf{x}) - H_1(\mathbf{v})(\mathbf{x})| &\leq \frac{1}{\epsilon^2 \omega_d} \int_{H_1(\mathbf{0})} J(|\xi|) (|\nabla^2 g'(\theta(\mathbf{x} + \epsilon \xi; \mathbf{u})) - \nabla^2 g'(\theta(\mathbf{x} + \epsilon \xi; \mathbf{v}))| \\ &\quad + |\nabla^2 g'(\theta(\mathbf{x}; \mathbf{u})) - \nabla^2 g'(\theta(\mathbf{x}; \mathbf{v}))|) d\xi. \end{aligned}$$

Let  $p_2(\mathbf{y})$ , where  $\mathbf{y} = \mathbf{x} + \epsilon \xi$  and  $\nabla$  is with respect to  $\mathbf{x}$ , is given by

$$(118) \quad p_2(\mathbf{y}) := |\nabla^2 g'(\theta(\mathbf{y}; \mathbf{u})) - \nabla^2 g'(\theta(\mathbf{y}; \mathbf{v}))|.$$

We then have

$$(119) \quad \|H_1(\mathbf{u}) - H_1(\mathbf{v})\|^2 \leq \left(\frac{1}{\epsilon^2}\right)^2 \frac{2\bar{J}_0}{\omega_d} \int_{H_1(\mathbf{0})} J(|\xi|) \left( \int_D (p_2(\mathbf{x} + \epsilon \xi)^2 + p_2(\mathbf{x})^2) dx \right) d\xi.$$

Note that

$$\nabla^2 g'(\theta(\mathbf{y}; \mathbf{u})) = g'''(\theta(\mathbf{y}; \mathbf{u})) \nabla \theta(\mathbf{y}; \mathbf{u}) \otimes \nabla \theta(\mathbf{y}; \mathbf{u}) + g''(\theta(\mathbf{y}; \mathbf{u})) \nabla^2 \theta(\mathbf{y}; \mathbf{u}).$$

We add and subtract terms to the equation above to get

$$\begin{aligned} &\nabla^2 g'(\theta(\mathbf{y}; \mathbf{u})) - \nabla^2 g'(\theta(\mathbf{y}; \mathbf{v})) \\ &= g'''(\theta(\mathbf{y}; \mathbf{u})) [\nabla \theta(\mathbf{y}; \mathbf{u}) \otimes \nabla \theta(\mathbf{y}; \mathbf{u}) - \nabla \theta(\mathbf{y}; \mathbf{v}) \otimes \nabla \theta(\mathbf{y}; \mathbf{v})] \\ &\quad + [g'''(\theta(\mathbf{y}; \mathbf{u})) - g'''(\theta(\mathbf{y}; \mathbf{v}))] \nabla \theta(\mathbf{y}; \mathbf{v}) \otimes \nabla \theta(\mathbf{y}; \mathbf{v}) \\ &\quad + g''(\theta(\mathbf{y}; \mathbf{u})) [\nabla^2 \theta(\mathbf{y}; \mathbf{u}) - \nabla^2 \theta(\mathbf{y}; \mathbf{v})] \\ &\quad + [g''(\theta(\mathbf{y}; \mathbf{u})) - g''(\theta(\mathbf{y}; \mathbf{v}))] \nabla^2 \theta(\mathbf{y}; \mathbf{v}). \end{aligned}$$

Using inequalities  $|g''(r)| \leq C_2^g$ ,  $|g'''(r)| \leq C_3^g$ ,  $|g''(r_1) - g''(r_2)| \leq C_3^g |r_1 - r_2|$ ,  $|g'''(r_1) - g'''(r_2)| \leq C_4^g |r_1 - r_2|$ , and  $|\mathbf{a} \otimes \mathbf{a} - \mathbf{c} \otimes \mathbf{c}| \leq (|\mathbf{a}| + |\mathbf{c}|) |\mathbf{a} - \mathbf{c}|$ , and the fact that  $\theta(\mathbf{y}; \mathbf{u}) - \theta(\mathbf{y}; \mathbf{v}) = \theta(\mathbf{y}; \mathbf{u} - \mathbf{v})$ , we have

$$\begin{aligned} p_2(\mathbf{y}) &\leq C_3^g |\nabla \theta(\mathbf{y}; \mathbf{u})| |\nabla \theta(\mathbf{y}; \mathbf{u} - \mathbf{v})| + C_3^g |\nabla \theta(\mathbf{y}; \mathbf{v})| |\nabla \theta(\mathbf{y}; \mathbf{u} - \mathbf{v})| \\ &\quad + C_4^g |\theta(\mathbf{y}; \mathbf{u} - \mathbf{v})| |\nabla \theta(\mathbf{y}; \mathbf{v})|^2 \\ &\quad + C_2^g |\nabla^2 \theta(\mathbf{y}; \mathbf{u} - \mathbf{v})| + C_3^g |\theta(\mathbf{y}; \mathbf{u} - \mathbf{v})| |\nabla^2 \theta(\mathbf{y}; \mathbf{v})|. \end{aligned}$$

Taking the square of the above equation and using  $(\sum_{i=1}^5 a_i)^2 \leq 5 \sum_{i=1}^5 a_i^2$  gives

$$\begin{aligned} \int_D p_2(\mathbf{y})^2 dx &\leq 5(C_3^g)^2 \int_D |\nabla \theta(\mathbf{y}; \mathbf{u})|^2 |\nabla \theta(\mathbf{y}; \mathbf{u} - \mathbf{v})|^2 dx \\ &\quad + 5(C_3^g)^2 \int_D |\nabla \theta(\mathbf{y}; \mathbf{v})|^2 |\nabla \theta(\mathbf{y}; \mathbf{u} - \mathbf{v})|^2 dx \\ &\quad + 5(C_4^g)^2 \int_D |\theta(\mathbf{y}; \mathbf{u} - \mathbf{v})|^2 |\nabla \theta(\mathbf{y}; \mathbf{v})|^4 dx \\ &\quad + 5(C_2^g)^2 \int_D |\nabla^2 \theta(\mathbf{y}; \mathbf{u} - \mathbf{v})|^2 dx \\ &\quad + 5(C_3^g)^2 \int_D |\theta(\mathbf{y}; \mathbf{u} - \mathbf{v})|^2 |\nabla^2 \theta(\mathbf{y}; \mathbf{v})|^2 dx \\ &=: I_1 + I_2 + I_3 + I_4 + I_5. \end{aligned}$$

We now estimate each term using [Lemma 10](#) as follows. Applying Hölder inequality and inequality [Equation 91](#) of [Lemma 10](#) to get

$$\begin{aligned} I_1 &\leq 5(C_3^g)^2 \left( \int_D |\nabla\theta(\mathbf{y}; \mathbf{u})|^4 d\mathbf{x} \right)^{1/2} \left( \int_D |\nabla\theta(\mathbf{y}; \mathbf{u} - \mathbf{v})|^4 d\mathbf{x} \right)^{1/2} \\ &\leq 640(C_3^g)^2 \bar{J}_0^4 (C_{e_2}^2 + C_{e_1} C_{\omega_1}^2)^2 \|\mathbf{u}\|_2^2 \|\mathbf{u} - \mathbf{v}\|_2^2. \end{aligned}$$

Similarly,

$$I_2 \leq 640(C_3^g)^2 \bar{J}_0^4 (C_{e_2}^2 + C_{e_1} C_{\omega_1}^2)^2 \|\mathbf{v}\|_2^2 \|\mathbf{u} - \mathbf{v}\|_2^2.$$

Using [Equation 92](#) of [Lemma 10](#), we get

$$I_3 \leq 2560(C_4^g)^2 \bar{J}_0^6 C_{e_1}^2 (C_{e_2}^2 + C_{e_1} C_{\omega_1}^2)^2 \|\mathbf{v}\|_2^4 \|\mathbf{u} - \mathbf{v}\|_2^2.$$

For  $I_4$ , we use inequality [Equation 93](#) to get

$$I_4 \leq 80(C_2^g)^2 \bar{J}_0^2 (1 + 2C_{\omega_1} + C_{\omega_2})^2 \|\mathbf{u} - \mathbf{v}\|_2^2.$$

In  $I_5$ , we use [Equation 87](#) and [Equation 93](#) to get

$$I_5 \leq 320 \bar{J}_0^4 C_{e_1}^2 (1 + 2C_{\omega_1} + C_{\omega_2})^2 \|\mathbf{v}\|_2^2 \|\mathbf{u} - \mathbf{v}\|_2^2.$$

After collecting results, we can find a constant  $L_5$  such that we have

$$(120) \quad \int_D p_2(\mathbf{y})^2 d\mathbf{x} \leq L_5^2 (1 + (\|\mathbf{u}\|_2 + \|\mathbf{v}\|_2) + (\|\mathbf{u}\|_2 + \|\mathbf{v}\|_2)^2) \|\mathbf{u} - \mathbf{v}\|_2^2.$$

We substitute [Equation 120](#) into [Equation 119](#) to show

$$\begin{aligned} \|H_1(\mathbf{u}) - H_1(\mathbf{v})\|^2 &\leq \frac{4L_5^2 \bar{J}_0^2 (1 + (\|\mathbf{u}\|_2 + \|\mathbf{v}\|_2) + (\|\mathbf{u}\|_2 + \|\mathbf{v}\|_2)^2)^2}{\epsilon^4} \|\mathbf{u} - \mathbf{v}\|_2^2 \\ \Rightarrow \|H_1(\mathbf{u}) - H_1(\mathbf{v})\| &\leq \frac{L_6 (1 + (\|\mathbf{u}\|_2 + \|\mathbf{v}\|_2) + (\|\mathbf{u}\|_2 + \|\mathbf{v}\|_2)^2)}{\epsilon^2} \|\mathbf{u} - \mathbf{v}\|_2 \\ (121) \quad &\leq \frac{L_6 (1 + \|\mathbf{u}\|_2 + \|\mathbf{v}\|_2)^2}{\epsilon^2} \|\mathbf{u} - \mathbf{v}\|_2 \end{aligned}$$

where we have introduced the new constant  $L_6$ .

We combine the estimates on  $H_1, H_2, H_3, H_4$ , introducing a new constant  $L_7$ , and get

$$(122) \quad \|\nabla^2 \mathcal{L}_D^\epsilon(\mathbf{u}) - \nabla^2 \mathcal{L}_D^\epsilon(\mathbf{v})\| \leq \frac{L_7 (1 + \|\mathbf{u}\|_2 + \|\mathbf{v}\|_2)^2}{\epsilon^2} \|\mathbf{u} - \mathbf{v}\|_2.$$

On adding the estimates [Equation 108](#), [Equation 113](#), [Equation 122](#) it is evident that the proof of [Theorem 1](#) is complete.

**6.2. Proof of higher temporal regularity.** In this section we prove that the peridynamic evolutions have higher regularity in time for body forces that are differentiable in time. To see this we take the time derivative of [Equation 11](#) to get a second order differential equation in time for  $\mathbf{v} = \dot{\mathbf{u}}$  given by

$$(123) \quad \rho \partial_{tt}^2 \mathbf{v}(\mathbf{x}, t) = Q(\mathbf{v}(t); \mathbf{u}(t))(\mathbf{x}) + \dot{\mathbf{b}}(\mathbf{x}, t),$$

where  $Q(\mathbf{v}; \mathbf{u})$  is an operator that depends on the solution  $\mathbf{u}$  of Equation 11 and acts on  $\mathbf{v}$ . It is given by,

$$(124) \quad Q(\mathbf{v}; \mathbf{u})(\mathbf{x}) = Q_T(\mathbf{v}; \mathbf{u})(\mathbf{x}) + Q_D(\mathbf{v}; \mathbf{u})(\mathbf{x}), \quad \forall \mathbf{x} \in D,$$

where

$$(125) \quad Q_T(\mathbf{v}; \mathbf{u})(\mathbf{x}) = \frac{2}{\epsilon^d \omega_d} \int_{H_\epsilon(\mathbf{x})} \omega(\mathbf{x}) \omega(\mathbf{y}) \frac{J^\epsilon(|\mathbf{y} - \mathbf{x}|)}{\epsilon |\mathbf{y} - \mathbf{x}|} \partial_{SS}^2 f(\sqrt{|\mathbf{y} - \mathbf{x}|} S(\mathbf{y}, \mathbf{x}, t; \mathbf{u})) S(\mathbf{y}, \mathbf{x}, t; \mathbf{v}) \mathbf{e}_{\mathbf{y} - \mathbf{x}} d\mathbf{y},$$

and

$$(126) \quad Q_D(\mathbf{v}; \mathbf{u})(\mathbf{x}) = \frac{1}{\epsilon^d \omega_d} \int_{H_\epsilon(\mathbf{x})} \omega(\mathbf{x}) \omega(\mathbf{y}) \frac{J^\epsilon(|\mathbf{y} - \mathbf{x}|)}{\epsilon^2} [\partial_{\theta\theta}^2 g(\theta(\mathbf{y}, t; \mathbf{u})) \theta(\mathbf{y}, t; \mathbf{v}) + \partial_{\theta\theta}^2 g(\theta(\mathbf{x}, t; \mathbf{u})) \theta(\mathbf{x}, t; \mathbf{v})] \mathbf{e}_{\mathbf{y} - \mathbf{x}} d\mathbf{y}.$$

Clearly, for  $\mathbf{u}$  fixed, the form  $Q(\mathbf{v}; \mathbf{u})$  acts linearly on  $\mathbf{v}$  which implies that the equation for  $\mathbf{v}$  is a linear nonlocal equation. The linearity of  $Q(\mathbf{v}; \mathbf{u})$  implies Lipschitz continuity for  $\mathbf{v} \in W$  as stated below.

**THEOREM 11. Lipschitz continuity of  $Q$**

Let  $\mathbf{u} \in W$  be any given field. Then for all  $\mathbf{v}, \mathbf{w} \in W$ , we have

$$(127) \quad \|Q(\mathbf{v}; \mathbf{u}) - Q(\mathbf{w}; \mathbf{u})\|_2 \leq \frac{L_8(1 + \|\mathbf{u}\|_2)^2}{\epsilon^3} \|\mathbf{v} - \mathbf{w}\|_2$$

where the constant  $L_8$  does not depend on  $\mathbf{u}, \mathbf{v}, \mathbf{w}$ . This gives for all  $\mathbf{v} \in W$  the upper bound,

$$(128) \quad \|Q(\mathbf{v}; \mathbf{u})\|_2 \leq \frac{L_8(1 + \|\mathbf{u}\|_2)^2}{\epsilon^3} \|\mathbf{v}\|_2.$$

The proof follows the same steps used in the proof of Theorem 1.

If  $\mathbf{u}$  is a peridynamic solution such that  $\mathbf{u} \in C^2(I_0; W)$  then we have for all  $t \in I_0$  the inequality

$$(129) \quad \|Q(\mathbf{v}; \mathbf{u}(t))\|_2 \leq \frac{L_8(1 + \sup_{s \in I_0} \|\mathbf{u}(s)\|_2)^2}{\epsilon^3} \|\mathbf{v}\|_2.$$

Note that Lipschitz continuity of  $\dot{\mathbf{u}}(t)$  stated in Theorem 2 implies  $\lim_{t \rightarrow 0^\pm} \partial_{tt}^2 \mathbf{u}(\mathbf{x}, t) = \partial_{tt}^2 \mathbf{u}(\mathbf{x}, 0)$ . We now demonstrate that  $\mathbf{v}(\mathbf{x}, t) = \partial_t \mathbf{u}(\mathbf{x}, t)$  is the unique solution of following initial boundary value problem.

**THEOREM 12. Initial value problem for  $\mathbf{v}(\mathbf{x}, t)$**

Suppose the initial data and righthand side  $\dot{\mathbf{b}}(t)$  satisfy the hypothesis of Theorem 2 and we suppose further that  $\dot{\mathbf{b}}(t)$  exists and is continuous in time for  $t \in I_0$  and  $\sup_{t \in I_0} \|\dot{\mathbf{b}}(t)\|_2 < \infty$ . Then  $\mathbf{v}(\mathbf{x}, t)$  is the unique solution to the initial value problem  $\mathbf{v}(\mathbf{x}, 0) = \mathbf{v}_0(\mathbf{x})$ ,  $\partial_t \mathbf{v}(\mathbf{x}, 0) = \partial_{tt}^2 \mathbf{u}(\mathbf{x}, 0)$ ,

$$(130) \quad \rho \partial_{tt}^2 \mathbf{v}(\mathbf{x}, t) = Q(\mathbf{v}(t); \mathbf{u}(t))(\mathbf{x}) + \dot{\mathbf{b}}(\mathbf{x}, t), \quad t \in I_0, \quad \mathbf{x} \in D,$$

$\mathbf{v} \in C^2(I_0; W)$  and

$$(131) \quad \|\partial_{tt}^2 \mathbf{v}(\mathbf{x}, t)\|_2 \leq \|Q(\mathbf{v}(t); \mathbf{u}(t))(\mathbf{x})\|_2 + \|\dot{\mathbf{b}}(\mathbf{x}, t)\|_2.$$

Theorem 3 now follows immediately from Theorem 12 noting that  $\partial_t \mathbf{u}(\mathbf{x}, t) = \mathbf{v}(\mathbf{x}, t)$  together with Equation 129 and Equation 131. The proof of Theorem 12 follows from the Lipschitz continuity Equation 127 and the Banach fixed point theorem as in [Brezis, 1983].

**7. Conclusions.** In this article, we have provided a-priori error estimates for finite element approximations to nonlocal state based peridynamic fracture models. We have shown that the convergence rate applies even over time intervals for which the material is softening over parts of the computational domain. The results are established for two different classes of state-based peridynamic forces. The convergence rate of the approximation is of the form  $C(\Delta t + h^2/\epsilon^2)$  where the constant  $C$  depends on  $\epsilon$  and the  $H^2$  norm of the solution and its time derivatives. For fixed  $\Delta t$  numerical simulations for Plexiglass show that the error decreases at the rate of  $h^2$  at  $40\mu$ -sec into the simulation. The simulations were carried out in parallel using 20 threads on a workstation with single Intel Xeon processor and with 32 GB of RAM. We anticipate similar convergence rates for longer times on bigger parallel machines.

We reiterate that the a-priori error estimates account for the possible appearance of nonlinearity anywhere in the computational domain. On the other hand numerical simulation and independent theoretical estimates show that the nonlinearity concentrates along “fat” cracks of finite length and width equal to  $\epsilon$ , see [Lipton, 2016, Lipton, 2014]. Moreover the remainder of the computational domain is seen to behave linearly and to leading order can be modeled as a linear elastic material up to an error proportional to  $\epsilon$ , see [Proposition 6, [Jha and Lipton 2018b]]. Future work will use these observations to focus on adaptive implementation and a-posteriori estimates.

## REFERENCES

- [Agwai et al., 2011] Agwai, A., Guven, I., and Madenci, E. (2011). Predicting crack propagation with peridynamics: a comparative study. *International journal of fracture*, 171(1):65–78.
- [Aksoylu and Unlu, 2014] Aksoylu, B. and Unlu, Z. (2014). Conditioning analysis of nonlocal integral operators in fractional sobolev spaces. *SIAM Journal on Numerical Analysis*, 52:653–677.
- [Bobaru and Hu, 2012] Bobaru, F. and Hu, W. (2012). The meaning, selection, and use of the peridynamic horizon and its relation to crack branching in brittle materials. *International journal of fracture*, 176(2):215–222.
- [Bobaru et al., 2016] Bobaru, F., Foster, J. T., Geubelle, P. H., Geubelle, P. H., and Silling, S. A. (2016). Handbook of peridynamic modeling.
- [Brenner and Scott, 2007] Brenner, S. and Scott, R. (2007). The mathematical theory of finite element methods, volume 15. *Springer Science & Business Media*, 3 edition.
- [Brezis, 1983] Brezis, H. (1983). Analyse fonctionnelle, théorie et application.
- [Chen and Gunzburger, 2011] Chen, X. and Gunzburger, M. (2011). Continuous and discontinuous finite element methods for a peridynamics model of mechanics. *Computer Methods in Applied Mechanics and Engineering*, 200(9):1237–1250.
- [Du, 2018a] Du, Q. (2018a). An invitation to nonlocal modeling, analysis and computation. *Proc. Int. Cong. of Math 2018*, Rio de Janeiro, Vol. 3 (3523-3552).
- [Du, 2018b] Du, Q. (2018b). Nonlocal modeling, analysis and computation. NSF-CBMS Monograph, SIAM Philadelphia (2018).
- [Du et al., 2013a] Du, Q., Gunzburger, M., Lehoucq, R., and Zhou, K. (2013a). Analysis of the volume-constrained peridynamic navier equation of linear elasticity. *Journal of Elasticity*, 113(2):193–217.
- [Du et al., 2013b] Du, Q., Ju, L., Tian, L., and Zhou, K. (2013b). A posteriori error analysis of finite element method for linear nonlocal diffusion and peridynamic models. *Mathematics of computation*, 82(284):1889–1922.
- [Du et al., 2013c] Du, Q., Tian, L., and Zhao, X. (2013c). A convergent adaptive finite element algorithm for nonlocal diffusion and peridynamic models. *SIAM Journal on Numerical Analysis*, 51(2):1211–1234.
- [Emmrich et al., 2013] Emmrich, E., Lehoucq, R. B., and Puhst, D. (2013). Peridynamics: a nonlocal continuum theory. In *Meshfree Methods for Partial Differential Equations VI*, pages 45–65. Springer.
- [Foster et al., 2011] Foster, J. T., Silling, S. A., and Chen, W. (2011). An energy based failure criterion for use with peridynamic states. *International Journal for Multiscale Computational Engineering*, 9(6).
- [Demengel, 2012] Demengel, F. (2012). Functional Spaces for the Theory of Elliptic Partial Differential Equations. *Universitext. Springer-Verlag London*, 1 edition.
- [Gerstle et al., 2007] Gerstle, W., Sau, N., and Silling, S. (2007). Peridynamic modeling of concrete structures. *Nuclear engineering and design*, 237(12):1250–1258.
- [Ghajari et al., 2014] Ghajari, M., Iannucci, L., and Curtis, P. (2014). A peridynamic material model for

- the analysis of dynamic crack propagation in orthotropic media. *Computer Methods in Applied Mechanics and Engineering*, 276:431–452.
- [Guan and Gunzburger, 2015] Guan, Q. and Gunzburger, M. (2015). Stability and accuracy of time-stepping schemes and dispersion relations for a nonlocal wave equation. *Numerical Methods for Partial Differential Equations*, 31(2):500–516.
- [Ha and Bobaru, 2010] Ha, Y. D. and Bobaru, F. (2010). Studies of dynamic crack propagation and crack branching with peridynamics. *International Journal of Fracture*, 162(1-2):229–244.
- [Jha and Lipton 2018b] Jha, P. K. and Lipton, R. (2018b). Numerical convergence of nonlinear nonlocal continuum models to local elastodynamics. *International Journal for Numerical Methods in Engineering*, 114(13):1389–1410.
- [Jha and Lipton, 2018a] Jha, P. K. and Lipton, R. (2018a). Numerical analysis of nonlocal fracture models in Hölder space. *SIAM J. Numer. Anal.*, 56: 906–941.
- [Jha and Lipton, 2019] Jha, P. K. and Lipton, R. (2019). Small horizon limit of state based peridynamic models. *In preparation*.
- [Jha and Lipton, 2017] Jha, P. K. and Lipton, R. (2017). Finite element approximation of nonlinear nonlocal models. *arXiv preprint arXiv:1710.07661*.
- [Karaa, 2012] Karaa, S. (2012). Stability and convergence of fully discrete finite element schemes for the acoustic wave equation. *Journal of Applied Mathematics and Computing*, 40(1-2):659–682.
- [Lipton, 2014] Lipton, R. (2014). Dynamic brittle fracture as a small horizon limit of peridynamics. *Journal of Elasticity*, 117:21–50.
- [Lipton, 2016] Lipton, R. (2016). Cohesive dynamics and brittle fracture. *Journal of Elasticity*, 124(2):143–191.
- [Lipton et al., 2018a] Lipton, R., Said, E., and Jha, P. (2018a). Free damage propagation with memory. *Journal of Elasticity*, 133(2):129–153.
- [Lipton et al., 2018b] Lipton, R., Said, E., and Jha, P. K. (2018b). Dynamic brittle fracture from nonlocal double-well potentials: A state-based model. *Handbook of Nonlocal Continuum Mechanics for Materials and Structures*, pages 1–27.
- [Lipton et al., 2016] Lipton, R., Silling, S., and Lehoucq, R. (2016). Complex fracture nucleation and evolution with nonlocal elastodynamics. *arXiv preprint arXiv:1602.00247*.
- [Littlewood, 2010] Littlewood, D. J. (2010). Simulation of dynamic fracture using peridynamics, finite element modeling, and contact. In *Proceedings of the ASME 2010 International Mechanical Engineering Congress and Exposition (IMECE)*.
- [Macek and Silling, 2007] Macek, R. W. and Silling, S. A. (2007). Peridynamics via finite element analysis. *Finite Elements in Analysis and Design*, 43(15):1169–1178.
- [Mengesha and Du, 2015] Mengesha, T. and Du, Q. (2015). On the variational limit of a class of nonlocal functionals related to peridynamics. *Nonlinearity*, 28(11):3999.
- [Ren et al., 2017] Ren, B., Wu, C., and Askari, E. (2017). A 3d discontinuous galerkin finite element method with the bond-based peridynamics model for dynamic brittle failure analysis. *International Journal of Impact Engineering*, 99:14–25.
- [Silling et al., 2010] Silling, S., Weckner, O., Askari, E., and Bobaru, F. (2010). Crack nucleation in a peridynamic solid. *International Journal of Fracture*, 162(1-2):219–227.
- [Silling, 2000] Silling, S. A. (2000). Reformulation of elasticity theory for discontinuities and long-range forces. *Journal of the Mechanics and Physics of Solids*, 48(1):175–209.
- [Silling and Bobaru, 2005] Silling, S. A. and Bobaru, F. (2005). Peridynamic modeling of membranes and fibers. *International Journal of Non-Linear Mechanics*, 40(2):395–409.
- [Silling et al., 2007] Silling, S. A., Epton, M., Weckner, O., Xu, J., and Askari, E. (2007). Peridynamic states and constitutive modeling. *Journal of Elasticity*, 88(2):151–184.
- [Silling and Lehoucq, 2008] Silling, S. A. and Lehoucq, R. B. (2008). Convergence of peridynamics to classical elasticity theory. *Journal of Elasticity*, 93(1):13–37.
- [Tian and Du, 2014] Tian, X. and Du, Q. Asymptotically compatible schemes and applications to robust discretization of nonlocal models. *SIAM J. Numer. Anal.*, 52-4 (2014), pp. 1641–1665.
- [Weckner and Abeyaratne, 2005] Weckner, O. and Abeyaratne, R. (2005). The effect of long-range forces on the dynamics of a bar. *Journal of the Mechanics and Physics of Solids*, 53(3):705–728.